Endocytosis of the damage-associated molecular pattern receptor PEPR1 is BAK1-dependent

Lucas Alves Neubus Claus[1,2,*], Fausto Andrés Ortiz-Morea[1,2,3,4], Shao-Li Yang[1,2], Shweta Yekondi[1,2], Xiangyu Xu[1,2], In-Cheol Yeo[3], Isabelle Vanhoutte[1,2], Nemanja Vukašinović[1,2], Qian Ma[1,2], Ive De Smet[1,2], Ping He[3], Libo Shan[3], and Eugenia Russinova[1,2,*]

[1]Department of Plant Biotechnology and Bioinformatics, Ghent University, 9052 Ghent, Belgium

[2]Center for Plant Systems Biology, VIB, 9052 Ghent, Belgium

[3]Department of Molecular, Cellular, and Developmental Biology, University of Michigan, Ann Arbor, Michigan 48109, USA

[4]Agricultural Engineering Program, University of the Amazon, Florencia 180002622, Colombia

Running title: BAK1 is required for PEPR1 internalization.

***Correspondence: Lucas Alves Neubus Claus (lucas.claus13@gmail.com) and Eugenia Russinova (eurus@psb.vib-ugent.be)**

ABSTRACT

After cellular damage caused by wounding or pathogens, *Arabidopsis thaliana* endogenous elicitor peptides (Peps) are released into the apoplast, enhancing innate immunity by directly binding to the membrane-localized leucine-rich repeat receptor kinase PEP RECEPTOR1 (PEPR1). Ligand binding induces PEPR1 heterodimerization with the co-receptor BRASSINOSTEROID INSENSITIVE1-ASSOCIATED KINASE1 (BAK1), followed by PEPR1 internalization, both essential for a subset of Pep1-induced responses. However, the role of BAK1 in Pep1-triggered PEPR1 endocytosis remains unclear. Here, we show that the ligand-induced PEPR1 endocytosis depends on its kinase activity and requires BAK1 C-terminal tail phosphorylation, which is equally indispensable for immune signaling and BAK1 internalization. Using a GFP insertional mutagenesis approach, we generated a partially functional GFP-tagged BAK1 to demonstrate that, following Pep1 elicitation, BAK1 and PEPR1 are endocytosed together with similar dynamics. Our findings identify the BAK1 function as a prerequisite for PEPR1 internalization.

Keywords: Arabidopsis, endogenous peptides, endocytosis, BAK1

39 **INTRODUCTION**

40

41 Damage-associated molecular patterns (DAMPs) are endogenous elicitor molecules released
42 into the apoplast after cell damage to trigger immune responses. An example of DAMPs in
43 plants is endogenous plant elicitor peptides (Peps) (Hou et al., 2019). Peps are 23-amino-acid
44 peptides that mature from a conserved C-terminal region of larger precursor proteins,
45 designated PROPEPs (Yamaguchi and Huffaker, 2011), which belong to a family of eight
46 members (PROPEP1 to PROPEP8) in *Arabidopsis thaliana* (Arabidopsis). Peps are recognized
47 by two homologous pattern recognition receptors (PRRs), the leucine-rich repeat (LRR)
48 receptor kinases (RKs) PEP RECEPTOR1 (PEPR1) and PEPR2 (Krol et al., 2010; Yamaguchi
49 et al., 2010; Bartels et al., 2013). The Pep-PEPR ligand-receptor pair is also present in other
50 dicots, such as *Solanaceae* and *Fabaceae* (Trivilin et al., 2014; Bartels and Boller, 2015), as
51 well as monocots, such as *Zea mays* (maize) (Huffaker et al., 2011, 2013).

52 Upon Pep1 binding, PEPR1 associates with the LRR co-receptor, BRASSINOSTEROID-
53 INSENSITIVE1 (BRI1)-ASSOCIATED RECEPTOR KINASE1 (BAK1)/SOMATIC
54 EMBRYOGENESIS RECEPTOR KINASE (SERK3), hereafter referred to as BAK1 (Tang et
55 al., 2015; Yamada et al., 2016). BAK1 is a promiscuous protein that regulates multiple signaling
56 pathways controlling growth, cell death, and innate immunity by forming ligand-dependent
57 complexes with several plasma membrane (PM)-localized RKs (Schulze et al., 2010;
58 Schwessinger et al., 2011). This raises the question of how BAK1 distinguishes between
59 different signaling pathways and responds accordingly. BAK1 has been shown to discriminate
60 between immune and brassinosteroid (BR) hormone responses in a phosphorylation-dependent
61 manner (Perraki et al., 2018). Accordingly, the *bak1-5* mutant allele, which carries a single
62 amino acid substitution (Cys to Tyr at position 408) in the kinase domain, leading to reduced
63 phosphorylation, is severely impaired in immune responses, but not in responses to BRs or cell
64 death (Schwessinger et al., 2011).

65 After perceiving Pep1, PEPR1 undergoes clathrin-mediated endocytosis (CME)
66 (Mbengue et al., 2016; Ortiz-Morea et al., 2016), an evolutionarily conserved process that is
67 essential for immunity and development in plants (Claus et al., 2018). CME regulates the
68 abundance of signaling components in the PM that are important for nutrient uptake (Takano
69 et al., 2010; Wang et al., 2017; Dubeaux et al., 2018), hormone signaling (Irani et al., 2012),
70 pathogen recognition, and stress responses (Krol et al., 2010; Choi et al., 2014). Previously,
71 PEPR1 was found to be internalized from the PM to the late endosome/multivesicular bodies
72 (LE/MVBs), bypassing the trans-Golgi network/early endosomes (TGN/EEs), from where it is

73 targeted to the vacuole for degradation (Ortiz-Morea et al, 2016). PEPR1 shares an
74 endomembrane trafficking pathway with the PRRs recognizing the microbe-associated
75 molecular patterns (MAMPs), such as FLAGELLIN-SENSING2 (FLS2) and EF-TU
76 RECEPTOR (EFR) (Robatzek et al., 2006; Mbengue et al., 2016), but differs from the well-
77 studied BR receptor BRI1, which is internalized from the PM to TGN/EE, where it can be
78 recycled back to the PM or targeted to the vacuole for degradation (Irani et al., 2012).

79 Endocytosis is often considered as a mechanism for removing receptors from the PM to
80 avoid continuous signaling that is potentially harmful to cells (Sigismund et al., 2012; Jaillais
81 and Vert, 2016). For example, in plants, blocking BRI1 endocytosis at the PM results in
82 constitutive BR responses, indicating that endocytosis attenuates BR signaling (Irani et al.,
83 2012; Martins et al., 2015; Zhou et al., 2018; Liu et al., 2020). However, disruption of PRR
84 endocytosis affects negatively plant defense responses (Ortiz-Morea et al., 2016; Mbengue et
85 al., 2016; Ekanayake et al., 2021).

86 Although considerable progress has been made in understanding the mechanisms of plant
87 receptor endocytosis, they remain poorly understood compared to their mammalian
88 counterparts. Post-translational modifications (PTMs), such as phosphorylation and
89 ubiquitination, are important regulators of FLS2 and BRI1 receptor endocytosis (Robatzek et
90 al., 2006; Mbengue et al., 2016; Lu et al., 2011; Martins et al., 2015; Zhou et al., 2018; Ma et
91 al., 2020). How the co-receptor BAK1 regulates endocytosis of the major receptors is still
92 unclear, because studies of BAK1 endocytosis in Arabidopsis have been hampered by the
93 observation that the C-terminally tagged BAK1 is not fully functional (Ntoukakis et al., 2011;
94 Lozano-Durán et al., 2013).

95 Here we sought to investigate the role of BAK1 in PEPR1 endocytosis. We found that, in
96 contrast to BRI1, the Pep1-induced endocytosis of PEPR1 requires BAK1 phosphorylation in
97 the C-terminal tail domain that is essential for both DAMP signaling and BAK1 endocytosis.
98 We further showed that the kinase activity of PEPR1 is necessary for its internalization and that
99 PEPR1 but not BAK1 was able to trans-phosphorylate *in vitro*. A GFP insertional mutagenesis
100 approach was used to generate a partially functional GFP-tagged BAK1, showing that following
101 Pep1 application BAK1 and PEPR1 are endocytosed together.

102

103 **RESULTS**

104

105 **Pep1-triggered responses are impaired by the C-terminal GFP-tagged BAK1 fusion**
106 **protein**

107 Arabidopsis plants expressing C-terminally tagged BAK1 variants exhibit impaired immune
108 responses to flg22 and elf18, but largely retain normal responses to exogenous BRs (Ntoukakis
109 et al., 2011; Lozano-Durán et al., 2013). Therefore, we tested whether the C-terminal tag of
110 BAK1 also interferes with responses to exogenous Pep1. To this end, we generated transgenic
111 Arabidopsis plants expressing native promoter-driven BAK1-GFP in the *bak1-4* mutant and
112 analyzed two independent transgenic lines (Supplemental Figure 1A-1E). BAK1-GFP
113 complemented the growth phenotype of *bak1-4* and remained functional in BR responses
114 (Supplemental Figure 1A-1E), although it caused slight BR hypersensitivity, possibly due to
115 increased expression levels (Supplemental Figure 1B and 1C). As previously described,
116 exogenous Pep1 inhibited wild-type root growth in a dose-dependent manner, whereas *bak1-4*
117 was hypersensitive to Pep1 (Figure 1A and 1B) due to sensitized PEPR signaling towards cell
118 death (Yamada et al., 2016). However, BAK1-GFP/*bak1-4* plants were insensitive to the Pep1-
119 induced root growth arrest, both MAPK activation and reactive oxygen species (ROS) burst
120 triggered by Pep1 were lower than in the wild-type, although the MAPK activation was less
121 affected (Figure 1C and 1D). Our findings indicate that, in addition to flg22 and elf18, the C-
122 terminal tag of BAK1 impairs Pep1 responses.
123
124 **BAK1 differentially regulates endocytosis of PEPR1 and BRI1**
125 Since exogenous Pep1 induces PEPR1 endocytosis (Ortiz-Morea et al., 2016), we tested
126 whether the C-terminally GFP-tagged BAK1 affects endocytosis of the Pep1-bound PEPR1 by
127 monitoring the internalization of the bioactive TAMRA-labelled Pep1 (TAMRA-Pep1) (Ortiz-
128 Morea et al., 2016) in BAK1-GFP/*bak1-4* plants (Figure 2A and 2B). As a control, we
129 quantified endocytosis of the fluorescent Alexa Fluor 647-castasterone (AFCS), a bioactive
130 fluorescently labelled BR analogue that is internalized together with BRI1 (Irani et al., 2012)
131 (Figure 2C and 2D). In contrast to the wild-type, TAMRA-Pep1 internalization was strongly
132 inhibited in BAK1-GFP/*bak1-4* plants, with few TAMRA-Pep1 puncta appearing inside the
133 cell and a strong signal remaining in the PM (Figure 2A and B). However, TAMRA-Pep1
134 internalization in the *bak1-4* mutant was not significantly different from that of the wild-type
135 at the analyzed time point (40 min chase) (Figure 2A and 2B). Consistently, exogenous Pep1-
136 induced PEPR1-GFP internalization in *bak1-4* and *pepr1pepr2* at 40 min (Supplemental Figure
137 2A) resembled TAMRA-Pep1 (Figure 2A and 2B) in both mutants but was partially inhibited
138 at later time points (60-120 min) in *bak1-4*. The AFCS uptake in BAK1-GFP/*bak1-4* and *bak1-*
139 *4* plants was comparable to or slightly higher than that of the wild-type (Figure 2C and 2D),

140 suggesting that C-terminally tagged BAK1 affects Pep1-PEPR1, but not AFCS-BRI1
141 endocytosis.
142 To confirm the importance of BAK1 for PEPR1 endocytosis, we examined the
143 internalization of PEPR1-GFP and TAMRA-Pep1 in different *serk* mutant combinations after
144 40 min chase (Supplemental Figure 2B-2E). TAMRA-Pep1 internalization was unaffected in
145 the *bak1-3serk4-1* double and the *serk1-1serk2-1serk4-1* triple mutant but was strongly
146 inhibited in the *serk1-1bak1-4* double mutant and the *serk1-1serk2-1bak1-4* triple mutant
147 (Supplemental Figure 2B-2E). These findings suggest that BAK1 and SERK1 redundantly
148 regulate PEPR1 endocytosis.
149 Taken together, our results show that C-terminally tagged BAK1 impairs ligand-induced
150 endocytosis of PEPR1 but not of BRI1, suggesting that BAK1 may regulate the internalization
151 of BR-bound BRI1 and Pep1-bound PEPR1 differently.
152
153 **The C-terminal phosphorylation of BAK1 is essential for PEPR1 endocytosis and**
154 **signaling**
155 Endocytosis of membrane proteins requires prior phosphorylation (Wang et al., 2017; Zhou et
156 al., 2018). The phosphorylation relationship between PEPR1 and BAK1 has not been
157 previously investigated. In vitro, the cytoplasmic domains (CDs) of both proteins displayed
158 autophosphorylation activity, although PEPR1 activity was weaker, whereas their respective
159 kinase-dead mutants (Km) were inactive (Supplemental Figure 3A and Supplemental Dataset
160 1). Notably, PEPR1-CD trans-phosphorylated BAK1-Km-CD, whereas BAK1-CD did not
161 trans-phosphorylate PEPR1-Km-CD, despite retaining the ability to trans-phosphorylate
162 BOTRYTIS-INDUCED KINASE 1 (BIK1)-Km (Lu et al., 2010) (Supplemental Figure 3B).
163 Mass spectrometry (MS) identified six PEPR1-mediated phosphorylation sites on BAK1 (S290,
164 T324, T446, T449, T450, and T455), four of which (T446, T449, T450, and T455) are located
165 in the activation loop (Supplemental Dataset 1). Furthermore, PEPR1-CD, but not PEPR1-Km-
166 CD, reduced BAK1 autophosphorylation *in vitro*, while the PEPR1-CD activity appeared
167 enhanced by BAK1-CD (Supplemental Figure 3A). A C-terminal cluster of BAK1
168 autophosphorylation sites (S602, T603, S604, and S612) is essential for a subset of its functions
169 (Perraki et al., 2018; Bender et al., 2021). Because, C-terminal GFP-tagged BAK1 loses
170 phosphorylation at one of these sites (S612) (Perraki et al., 2018), we hypothesized that this
171 cluster is critical for Pep1-PEPR1 endocytosis and signaling. To test this, we compared
172 TAMRA-Pep1 uptake in the phosphorylation-deficient $BAK1^{S612A}$ and $BAK1^{S602AT603AS604A}$
173 (hereafter $BAK1^{AAA}$) mutants with wild-type. Both mutants showed markedly reduced uptake,

174 with a more pronounced effect in BAK1^{S612A} (Figure 3A and 3B). Similarly, of PEPR1-GFP
175 endocytosis was impaired in both phosphorylation-deficient BAK1 variants expressed in the
176 *bak1-4* background, again with a stronger reduction in the BAK1^{S612A} mutant (Figure 3C and
177 3D).

178 Since PEPR1-Pep1 endocytosis was impaired in the BAK1^{S612A} and BAK1^{AAA} mutants,
179 we suspected that the Pep1-induced signaling would also be disturbed. To test this hypothesis,
180 we performed root growth, MAPK activation and ROS burst assays after Pep1 treatment (Figure
181 4; Supplemental Figure 4). Similar to BAK1-GFP/*bak1-4*, BAK1^{S612A}/*bak1-4* and
182 BAK1^{AAA}/*bak1-4* plants were strongly insensitive to Pep1 treatment (Figure 4A and 4B) and
183 both MAPK activation (Figure 4C) and ROS burst were reduced compared to the wild-type
184 (Figure 4D). To further confirm that BAK1 phosphorylation is crucial for Pep1-induced
185 endocytosis, we analyzed the *bak1-5* mutant, which carries the C408Y point mutation,
186 responsible for the BAK1 hypoactivity (Schwessinger et al., 2011). *bak1-5* resembled BAK1-
187 GFP/*bak1-4*, BAK1^{S612A}/*bak1-4*, and BAK1^{AAA}/*bak1-4* plants in that it was less responsive to
188 exogenous Pep1 in the root growth inhibition assay (Supplemental Figure 5A and 5B),
189 consistent with previous findings for the MAMPs flg22 and elf18 (Schwessinger et al., *2*011).
190 Additionally, Pep1-PEPR1 endocytosis was impaired in *bak1-5* mutant (Supplemental Figure
191 5C and 5D). Taken together, our results indicate that C-terminal BAK1 phosphorylation, which
192 is indispensable for flg22, elf18, and Pep1 signaling, is also a prerequisite for Pep1-induced
193 PEPR1 endocytosis.
194

195 **Pep1 endocytosis requires kinase-active PEPR1**

196 To investigate whether phosphorylation of PEPR1 after ligand binding is required for its
197 internalization, we generated transgenic plants expressing a kinase-dead PEPR1-GFP (PEPR1-
198 Km-GFP) in the *pepr1pepr2* double mutant (Figure 5A). As previously reported (Ortiz-Morea
199 et al., 2016), without elicitation, PEPR1-GFP localized mainly to the PM, with a few puncta
200 inside the cell. Pep1 treatment triggered its internalization, with an endocytosis peak after
201 40 min. However, endocytosis of PEPR1-Km-GFP after Pep1 application was decreased, and
202 the delay was most apparent 90-120 min after elicitation, when the fluorescence signal almost
203 disappeared, although the PM signal remained stronger. Interestingly, without exogenous Pep1,
204 PEPR1-Km-GFP was observed in intracellular puncta, possibly indicating either endocytosis
205 of PEPR1-Km-GFP without ligand binding or increase of its *de novo* production and exocytosis
206 (Figure 5A). To further investigate, we treated PEPR1-GFP and PEPR1-Km-GFP plants with
207 Brefeldin A (BFA), an indirect inhibitor of endosomal trafficking, that induces aggregation of

208 the *trans*-Golgi network/early endosome (TGN/EE) compartments, forming BFA bodies
209 (Geldner et al., 2003) (Figure 5B). Without Pep1 elicitation, PEPR1-GFP was only weakly
210 present in the BFA bodies, but after Pep1 application, PEPR1-GFP puncta were excluded from
211 the BFA bodies and localized to the periphery of the TGN/EE aggregates. Notably, under both
212 Pep1-treated or mock conditions, the PEPR1-Km-GFP labelling of the BFA bodies was strong,
213 suggesting that the BFA bodies accumulate both internalized and secreted PEPR1-Km-GFP
214 (Figure 5B).
215 Cycloheximide (CHX), which blocks *de novo* protein synthesis, is routinely used to avoid
216 the interference from secreted proteins when analyzing endocytosis or recycling (Liu et al.,
217 2020). Unexpectedly, CHX blocked PEPR1 internalization (Supplemental Figure 6A) and
218 disturbed the Pep1-triggered MAPK activation (Supplemental Figure 6B). To overcome this
219 limitation, we used TAMRA-Pep1, which allows the tracking of PEPR1 internalization from
220 the PM. In contrast to PEPR1-GFP, the endocytosis of PEPR1-Km-GFP was reduced after
221 TAMRA-Pep1 application (Figure 5C). After BFA treatment, TAMRA-Pep1 does not label the
222 BFA bodies in plants expressing either PEPR1-GFP or PEPR1-Km-GFP, indicating that the
223 accumulated PEPR1-Km-GFP signal in the BFA bodies is mainly due to newly protein
224 synthesis and exocytosis (Figure 5C). Thus, PEPR1 kinase activity is required for its
225 endocytosis.
226
227 **BAK1 and PEPR1 are co-internalized**
228 To investigate whether BAK1 is internalized together with PEPR1 we used an insertional GFP
229 mutagenesis approach to generate a functional BAK1-GFP fusion by inserting the GFP at
230 different positions into the BAK1 protein (Supplemental Figure 7A and 7B). All constructs
231 were introduced into the *bak1-4* null mutant under the control of the *BAK1* promoter and several
232 independent transgenic lines of each construct were analyzed. Two constructs with GFP
233 insertions into BAK1 between the juxta membrane and the kinase domains (BAK1K253-GFP
234 and BAK1Q273-GFP) and two constructs in which the GFP was inserted into the C-terminal
235 tail of BAK1 (BAK1M580-GFP and BAK1A593-GFP) were selected (Supplemental Figures
236 1A-1C and 8A-8B). Of all transgenic lines initially tested in a Pep1-induced root growth
237 inhibition assay, only BAK1K253-GFP and BAK1Q273-GFP partially recovered from the
238 Pep1-triggered root inhibition, although they remained more sensitive to Pep1 than plants
239 expressing the C-terminally tagged BAK1. This phenotype was confirmed with different Pep1
240 concentrations (Figure 6A and 6B and Supplemental Figure 8C-8E). However, Pep1-triggered
241 MAPK activation in BAK1K253-GFP and BAK1Q273-GFP plants was similar to that of plants

242 expressing BAK1-GFP (Figure 6C). The two mutant lines were more responsive to Pep1
243 application in terms of ROS burst, although they did not produce the ROS levels of the wild-
244 type (Figure 6D). We further examined the responses of these lines to exogenous BRs by
245 assessing the hypocotyl elongation in the dark and the accumulation of dephosphorylated BES1
246 (dBES1), which serves as a readout for BR signaling activation (Yin et al., 2002) (Supplemental
247 Figure 1F and 1G). The hypocotyl growth of BAK1K253-GFP and BAK1Q273-GFP seedlings
248 was sensitive to 100 nM, but not 10 nM brassinolide (BL) and the BES1 dephosphorylation
249 levels were similar to those of the wild-type and BAK-GFP expressing plants, suggesting that
250 the response to exogenous BRs in these lines was not notably affected by the GFP tag.

251 Next, we took advantage of the partially functional BAK1K253-GFP and BAK1Q273-
252 GFP constructs to analyze TAMRA-Pep1 uptake in the corresponding Arabidopsis transgenic
253 plants (Figure 7A and 7B). Interestingly, the endocytosis of TAMRA-Pep1 was restored in
254 BAK1K253-GFP and BAK1Q273-GFP plants compared to BAK1-GFP (Figure 7A and 7B).
255 After a 40-minute chase, TAMRA-Pep1 accumulated in the PM of plants expressing BAK1-
256 GFP, whereas it was clearly internalized in plants expressing BAK1K253-GFP and
257 BAK1Q273-GFP. Based on the recovery of PEPR1 endocytosis in the BAK1K253-GFP and
258 BAK1Q273-GFP lines, we hypothesized that PEPR1 and BAK1 are endocytosed together.
259 Therefore, we analyzed the co-localization between BAK1-GFP and TAMRA-Pep1 (Figure 7C
260 and 7D). Both BAK1K253-GFP and BAK1Q273-GFP co-localized with the TAMRA-Pep1
261 after a 40-minute chase, though not all TAMRA-Pep1 puncta contained the BAK1-GFP (Figure
262 7C). Furthermore, AFCS uptake experiments confirmed that BRI1 endocytosis was not
263 impaired in the BAK1K253-GFP and BAK1Q273-GFP lines (Figure 7E and 7F), consistent
264 with our observations that BR signaling remained unaffected in these plants.

265 To confirm that BAK1 and PEPR1 are internalized together, we purified clathrin-coated
266 vesicles (CCVs) from Arabidopsis *pRPS5A-PEPR1-GFP*/*pepr1pepr2* seedlings and examined
267 whether BAK1 was present alongside PEPR1 in the enriched CCV fractions after treatment
268 with Pep1 (500 nM for 20 min). Whole Arabidopsis seedlings were used for the isolation of
269 CCVs because Pep1 induced triggered PEPR1-GFP endocytosis in both shoots and roots
270 (Supplemental Figure 9). Analysis of the enriched CCV fractions by immunoblotting revealed
271 that BAK1 was barely detectable in the mock treatment but was enriched in CCVs after Pep1
272 treatment, as was PEPR1 (Figure 7G). Taken together, our data indicate that BAK1 and PEPR1
273 are likely endocytosed together.

274

275 **DISCUSSION**

276

277 Endocytosis controls the amount of functional cell surface receptors and their ligands, acting as
278 a spatial and temporal organizer of signaling (Sigismund et al., 2012). A link between
279 endocytosis and signaling has been established for several Arabidopsis RKs involved in
280 development and immunity (Erwig et al., 2017; Irani et al,. 2012; Mbengue et al., 2016; Ortiz-
281 Morea et al., 2016). BAK1 and other SERK family members function as co-receptors (Fan et
282 al., 2016), but experimental evidence for their involvement in the endocytosis of the main
283 receptors is still lacking.

284 Transient expression analyses of BAK1 subcellular dynamics in cowpea mesophyll
285 protoplasts (Russinova et al, .2004; Song et al., 2009) revealed that the C-terminal GFP-tagged
286 BAK1 cycles between the PM and the endosomes. Surprisingly, similar dynamics was not
287 observed in Arabidopsis roots (Bücherl et al., 2013), although, BAK1-GFP localized in the PM,
288 and was able to complement the BR-related defects of the *bak1-4* null mutant (Ntoukakis et al.,
289 2011; Lozano-Durán et al., 2013). Further assessment of BAK1 subcellular dynamics has been
290 hampered by the observation that the C-terminal GFP-tagged BAK1 is unable to respond to
291 exogenous flg22 and elf18 (Ntoukakis et al., 2011; Lozano-Durán et al., 2013). Here, we show
292 that BAK1-GFP is also impaired in Pep1-triggered responses. Disruption of protein
293 functionality due to a tag fusion has been previously reported in both plant and mammalian
294 systems (Wiśniewska et al., 2006; Hammond et al., 2010; Hurst et al., 2018) and can potentially
295 lead to misinterpretation of the results. Moreover, the functionality of protein fusions may
296 depend on the protein complexes and their respective functions. One possible explanation for
297 the impaired immune responses caused by the C-terminal GFP tag of BAK1 is that it may act
298 in a dominant-negative manner, thereby interfering with receptor complex activation or
299 downstream signal transduction. For example, it could disrupt the recruitment of certain protein
300 partners to the receptor complex, affect PTMs crucial for signaling, or, similar to BAK1-5
301 protein, stabilize the PEPR1-BAK1 complex at the PM (Schwessinger et al., 2011). Consistent
302 with this, the C-terminal GFP tag was found to impede the phosphorylation on S612 in the C-
303 terminal tail of BAK1, the domain specifically targeted by phosphorylation events required to
304 trigger immune responses in Arabidopsis in response to flg22 and elf18 (Perraki et al., 2018).
305 Additionally, $BAK1^{S612A}$ appeared to co-purify with more FLS2 than the wild-type BAK1
306 (Perraki et al., 2018). Remarkably, Pep1-induced PEPR1 endocytosis was also severely
307 impaired in the transgenic lines expressing the C-terminal GFP-tagged BAK1, whereas the
308 BRI1-dependent internalization of AFCS remained unaffected. Furthermore, $BAK1^{AAA}$ and
309 $BAK1^{S612A}$ mutants deficient in conserved phosphorylation sites, significantly reduced Pep1-

310 induced PEPR1 internalization, providing evidence that BAK1 phosphorylation, necessary for
311 the immune responses (Perraki et al., 2018), is also important for Pep1-triggered PEPR1
312 endocytosis. Supporting this, the semi-dominant *bak1-5* mutant, known to disrupt the immune
313 phosphorylation-dependent function of BAK1 (Perraki et al., 2018), strongly blocked Pep1-
314 triggered PEPR1 endocytosis. Moreover, PEPR1 internalization was only slightly disturbed in
315 the *bak1-4* null mutant, but severely affected in the *bak1-4serk1-1* mutants, suggesting that
316 BAK1 and SERK1 redundantly regulate PEPR1 endocytosis, consistent with earlier studies in
317 tobacco (Mbengue et al., 2016).

318 Examination of the co-localization between the C-terminal GFP-tagged BAK1 and
319 TAMRA-Pep1 revealed that BAK1 localized to the PM, but it did not label the positive
320 compartments of TAMRA-Pep1. This suggest that BAK1 dynamics may be a prerequisite for
321 PEPR1, but not BRI1, endocytosis and signaling, consistent with observations that the C-
322 terminal GFP-tagged BAK1 was functional in terms of BR responses (Ntoukakis et al., 2011;
323 Lozano-Durán et al., 2013). To support this hypothesis and overcome the lack of immune
324 responses caused by the C-terminal GFP tag, we applied an insertional GFP approach to identify
325 a functional fluorescently tagged BAK1 for subcellular dynamics studies. Since the C-terminal
326 tail of BAK1 is important for immune signaling (Wu et al., 2018; Perraki et al., 2018), we
327 inserted the GFP before the critical residues within the C-terminal tail for the generation of
328 BAK1M580-GFP and BAK1A593-GFP, and between the JMD and the KD for that of
329 BAK1K253-GFP and BAK1Q273-GFP.

330 Remarkably, both BAK1K253-GFP and BAK1Q273-GFP versions retained partial
331 responses to exogenous BRs and Pep1, showed dynamics, and restored PEPR1 endocytosis. In
332 addition, BAK1K253-GFP and BAK1Q273-GFP co-localized with TAMRA-Pep1 puncta,
333 suggesting that PEPR1 is endocytosed together with BAK1. Consistent with this co-
334 localization, BAK1 and PEPR1 were detected together in isolated CCVs from Arabidopsis
335 plants after Pep1 treatment. The fact that BAK1 is endocytosed together with PEPR1 raises the
336 possibility that the BAK1-PEPR1 receptor complex maintains signaling from endosomes
337 (Figure 8). In mammals, the role of endosomes as signaling platforms is a well-studied, albeit
338 still controversial, phenomenon (Pavlos and Friedman, 2017). However, conclusive evidence
339 for endosomal signaling in plants is still lacking. Further study of the internalization and
340 dynamics of the PEPR1-BAK1 receptor complex may provide additional proof for the existence
341 of similar mechanisms in plants.

342 The ligand-induced endocytosis of PEPR1 depended on its kinase activity, but the
343 phosphorylation relationship between BAK1 and PEPR1 is unclear. Protein kinases lacking

344 Arginine in the catalytic loop HxD motif, also known as non-RD kinases, are implicated in
345 immune signaling and may be activated by phosphorylation-dependent conformational changes
346 in the receptor cytoplasmic domain, but not by an activation loop phosphorylation (Bender et
347 al., 2021). For example, BAK1 phosphorylates the non-RD kinase EFR in the activation loop
348 to stabilize its active conformation, allowing EFR in turn to allosterically activate BAK1 but
349 not vice versa (Wang et al., 2014; Schwessinger et al., 2011; Mühlenbeck et al., 2024). Unlike
350 other PRRs, PEPR1 is an RD kinase with strong kinase activity *in vitro* and has been shown to
351 phosphorylate various partners, such as BIK1 (Liu et al., 2013) and the REGULATOR OF G
352 SIGNALLING PROTEIN1 (RGS1) (Tunc-Ozdemir et al., 2017). BAK1 can trans-
353 phosphorylate most of its co-receptors, including the non-RD kinases FLS2 (Lin et al., 2014),
354 EFR (Wang et al., 2014; Schwessinger et al., 2011), the RD kinase BRI1 (Wang et al., 2008),
355 and other substrates, such as NUCLEAR SHUTTLE PROTEIN-INTERACTING KINASE1
356 (NIK1) (Li et al., 2019), BIK1 (Liu et al., 2017), and H^+-ATPASE ISOFORM2 (AHA2) (Pei
357 et al., 2022). We found that PEPR1 can phosphorylate BAK1 *in vitro*, but, surprisingly, BAK1
358 did not phosphorylate PEPR1 *in vitro* and *in vivo* (Supplemental Figure 3B; Supplemental
359 Dataset 2). However, the presence of the BAK1 kinase visibly increased PEPR1
360 phosphorylation *in vitro*, comparable to the observed *in vivo* increase in phosphorylation at
361 T896 in PEPR1 when co-expressed with BAK1 in the presence of Pep1 in tobacco
362 (Supplemental Dataset 2). Additionally, PEPR1 kinase reduced BAK1 phosphorylation *in vitro*.
363 Likewise, FLS2 and EFR reduced BAK1 kinase activity *in vitro* (Wang et al., 2014). Taken
364 together, the mutual trans-phosphorylation mechanism for activation of RKs complexes, as in
365 BRI1-BAK1 and FLS2-BAK1, might not apply to PEPR1-BAK1 and requires further
366 investigation.

367 In conclusion, our study demonstrates that the PEPR1 endocytosis is controlled by the
368 co-receptor BAK1 via phosphorylation in its C-terminal tail, which is indispensable for Pep1-
369 mediated signaling. This raises the question of the possible mechanism underlying this
370 regulation (Figure 8). It is tempting to speculate that BAK1 counteracts an as-yet-unknown
371 component of the receptor complex that negatively regulates PEPR1 endocytosis. In line with
372 this hypothesis, BAK1 restricts the activation of the LRR RK, BAK-TO-LIFE 2 (BTL2)
373 through specific phosphorylation to maintain cellular integrity (Yu et al., 2023). However,
374 whether BTL2 affects endocytosis of the main receptor remains unclear. BAK1 can also
375 regulate specific PTMs in PEPR1 that positively regulate ligand-induced receptor endocytosis,
376 such as phosphorylation or ubiquitination (Dubeaux and Vert, 2017). Notably, in contrast to
377 other BAK1 receptor partners, PEPR1 can phosphorylate BAK1 to reduce its activity.

378 Additionally, the immune-required phosphorylation of BAK1 is not necessary for BRI1
379 endocytosis, suggesting that BAK1 employs different mechanisms to regulate different receptor
380 partners. Nevertheless, the precise mechanism by which BAK1 controls PEPR1 endocytosis
381 remains to be elucidated. Whether BAK1 has a similar effect on other PRRs is unclear. Some
382 conflicting evidence exists that BAK1 is essential for ligand-induced endocytosis of certain
383 PRRs in transient assays (Mbengue et al., 2016), but it is not required for FLS2 recycling in
384 Arabidopsis leaves, regardless of the ligand presence (Beck et al., 2012). Furthermore, using
385 the newly designed and partially functional BAK1-GFP lines, it would be interesting to
386 investigate BAK1 dynamics within different immune receptor complexes, such as FLS2 and
387 EFR. Our findings suggest that the ligand-induced endocytosis of the main receptor is regulated
388 in a co-receptor-dependent manner.
389
390 **METHODS**
391
392 **Plant material, growth conditions and reagents**
393 All mutants and transgenic lines used in this study were in the background of the *Arabidopsis*
394 *thaliana* (L.) Heynh. (accession Columbia-0 [Col-0]). Seeds were surface-sterilized with
395 chlorine gas and then placed on plates with half-strength Murashige and Skoog (½MS) medium
396 containing 0.8% (w/v) agar, and 2.5 mM methyl ester sulfonate at pH 5.7. After vernalization
397 for 2 days at 4°C, the plates were moved to the growth chamber at 22°C in a 16 h/8 h light/dark
398 cycle with a light intensity of 120 μE m^{-2} s^{-1}. The following mutant and transgenic Arabidopsis
399 lines have been described previously: *pRPS5A-PEPR1-GFP/pepr1pepr2* (Ortiz-Morea *et al*,
400 2016); *bak1-4* (Chinchilla *et al*, 2007); *bak1-5* (Schwessinger *et al*, 2011); *serk1-1bak1-4*
401 (Meng *et al*, 2015); *bak1-3/serk4-1* (Du *et al,* 2016); *serk1-1(+/-)serk2-1bak1-4* (Meng *et al*,
402 2015); *serk1-1serk2-1(+/-)serk4-1* (Meng *et al*, 2015); *pBAK1-BAK1/bak1-4* (Perraki *et al*,
403 2018); *pBAK1-BAK1*^{S612A}*/bak1-4* (Perraki *et al*, 2018); and *pBAK1-BAK1*$^{S602A;T603A;S604A}$*/bak1-*
404 *4* (Perraki *et al*, 2018). The *pRPS5A-PEPR1-GFP* construct (Ortiz-Morea *et al*, 2016) was
405 introduced into the *bak1-4* mutant (Chinchilla *et al*, 2007) by Agrobacterium-mediated
406 transformation. The *pRPS5A-PEPR1-GFP/pBAK1-BAK1*^{S612A}*/bak1-4* and *pRPS5A-PEPR1-*
407 *GFP/pBAK1-BAK1*$^{S602A;T603A;S604A}$*/bak1-4* lines were generated by crossing *pRPS5A-PEPR1-*
408 *GFP/bak1-4* with either *pBAK1-BAK1*^{S612A}*/bak1-4* or *pBAK1-BAK1*$^{S602A;T603A\ ;S604A}$*/bak1-4*. For
409 phenotypic analysis, plants were grown in soil in a growth chamber at 22°C, 58% relative
410 humidity, and a 16 h light/8 h light/dark photoperiod for 6 weeks. N-(3-
411 triethylammoniumpropyl)-4-(6-(4-(diethylamino) phenyl) hexatrienyl) pyridinium dibromide

412 (FM4-64; 2 mM stock in purified water; Invitrogen), BFA [50 mM stock in dimethyl sulfoxide
413 (DMSO); Sigma-Aldrich], CHX (50 mM stock in DMSO; Sigma-Aldrich), BL (10 mM stock
414 in DMSO; Wako Pure Chemical Industries and OlChemlm) were used at the concentrations
415 indicated in the figure legends.
416
417 **Plasmid construction**
418 cDNA or genomic DNA from Arabidopsis Col-0 was used as template for PCR cloning. The
419 *BAK1* promoter was amplified and introduced into the *pDONRP4-P1R* donor vector to build
420 *pDONRP4-P1R-pBAK1*. The *BAK1* coding sequence without stop codon was cloned into
421 *pDONR221* to generate *pDONR221-BAK1* that was used as a template together with
422 *pDONRP2-P3R-GFP* to generate the BAK1 insertional GFP versions by overlapping PCR and
423 subcloned into *pDONR221* to generate *pDONRP1P2-BAK1K253-GFP, pDONRP1P2-*
424 *BAK1Q273-GFP, pDONRP1P2-BAK1M580-GFP* and *pDONRP1P2-BAK1A593-GFP.* The
425 destination vectors were generated by recombining the *pH7m24GW,3, pDONRP4-P1R-pBAK1,*
426 and *pDONRP1P2-BAK1-GFP* versions.
427 For protein purification, the CD-encoding sequences of BAK1were amplified and
428 introduced into *pDONR221* to generate *pDONR221-BAK1-CD* that was used as template to
429 generate *BAK1-Km(D416N)-CD* by overlapping PCR and subcloned into *pDONR221*. The
430 entry clones *pDONR221-BAK1-CD* and *pDONR221-BAK1-Km-CD* were recombined into the
431 bacterial expression vector *pOPINM* (Berrow *et al*, 2007) containing the His6-MBP tag.
432 Sequences encoding CDs of *PEPR1* and *PEPR1-Km(K855E)* were amplified with specific
433 primers containing restriction sites. The point mutations were generated by means of
434 overlapping PCR. The PCR products and the plasmid *pGEX-5x1* were digested with the
435 restriction enzymes EcoRI and BamHI (FastDigest; Thermo Fisher Scientific). The linearized
436 and purified plasmid was dephosphorylated by Thermosensitive Alkaline Phosphatase
437 (Promega). PCR products and plasmid were ligated by T4 DNA ligase (Invitrogen) to generate
438 *pGEX-5x1-PEPR1-CD* and *pGEX-5x1-PEPR1-Km-CD*. Constructs were introduced into the
439 *Escherichia coli* strain Rosetta2 for protein production. All primers used are listed in Table
440 EV1. All clones were confirmed by sequencing.
441
442 **Generation of transgenic plants**
443 Plants were transformed with the *Agrobacterium tumefaciens* strain C58C1 by means of the
444 floral dip method (Clough & Bent, 1998). BAK1 constructs were transformed into the *bak1-4*

445 null mutant Transformed plants were selected on ½MS agar medium containing 50 mg/l
446 hygromycin.
447
448 **Peptides**
449 The peptide Pep1 (ATKVKAKQRGKEKVSSGRPGQHN) with a HPLC purity of 95% and the
450 peptide Pep1 labelled with 5'- carboxytetramethylrhodamine at the N-terminal (TAMRA-Pep1)
451 with a HPLC purity of 95% were purchased from EZBiolab. The peptides were dissolved in
452 water to obtain peptide stocks of 1 mM and further diluted with ½MS medium.
453
454 **Root and hypocotyl growth assays**
455 Seeds were sown on ½MS solid medium, stratified for 2 days at 4°C in the dark, and placed
456 vertically in the light. Four days after germination, seedlings were transferred to solid ½MS
457 medium supplemented with or without the indicated amount of Pep1 and incubated for a further
458 3 days, whereafter the plates were scanned. For the hypocotyl, seeds were sown directly on ½
459 MS medium supplemented with either increasing concentrations of BL or (DMSO), stratified
460 for 2 days at 4ºC in the dark. The plates were moved to growth chamber at 22ºC and placed
461 vertically in light for 6 h. Then, the plates were wrapped in aluminum foil for dark condition
462 and kept vertically in growth chamber at 22°C for 5 days. For root and hypocotyl
463 measurements, plates were scanned and the scanned images were processed and evaluated with
464 the ImageJ software and plotted relative to the untreated control.
465
466 **Detection of reactive oxygen species (ROS) burst**
467 For ROS burst assay (Zhang *et al*, 2010), leaf discs (5 mm in diameter) were collected from the
468 third or fourth true leaves of four-week-old Arabidopsis plants grown in soil. These discs were
469 placed into individual wells of a 96-well plate, each containing 100 µL of distilled water, and
470 left to incubate overnight under a 12-hour light/12-hour dark cycle. The next day, the water was
471 replaced with 100 µL of a reaction solution composed of 50 µM luminol and 10 µg/mL
472 horseradish peroxidase (Sigma-Aldrich, USA), with or without the addition of Pep1 at
473 concentrations as indicated. Luminescence signals were detected using a GloMax-Multi System
474 luminometer (Promega, USA).
475
476 **MAP kinase assay**
477 Arabidopsis seedlings were germinated on ½ MS medium and, after three or five days, were
478 transferred to a 12-well plate with ½ MS medium. Following 1 hour of conditioning, the

479 medium was supplemented with 100 nM Pep1. Seedlings were incubated with peptides for the
480 indicated time points, whereafter they were harvested and frozen in liquid N_2. Frozen plant
481 material was ground and the extraction buffer [50 mM Tris, pH 7.5, 200 mM NaCl, 1 mM
482 EDTA, 10% (v/v) glycerol, 0.1% (v/v) Tween 20, 1 mM phenylmethylsulfonyl fluoride, 1 mM
483 DTT, 1×PhosSTOP™ (4906837001; Sigma-Aldrich) and 1×cOmplete™ ULTRA Tablets
484 (5892791001; Sigma-Aldrich)] was added at the ratio of 2 µL per mg tissue (1:2 w:v). Samples
485 were vortexed and centrifuged at 13000*g* for 30 min. Protein concentration was quantified in
486 the supernatant with the Qubit protein assay kit (Thermo Fischer Scientific). Equal amounts of
487 proteins (30 µg) were separated on 7.5% sodium dodecyl sulphate (SDS)/polyacrylamide gel
488 electrophoresis (PAGE) and transferred onto a nitrocellulose membrane (Bio-Rad). After
489 blocking with 3% bovine serum albumin, membranes were incubated overnight with primary
490 antibodies against anti-phospho- p44/42 (1:2500; Cell Signaling Technology). Horseradish
491 peroxide (HRP)-conjugated anti-rabbit secondary antibody (1:10000; GE Healthcare;) was used
492 and signals were detected with the SuperSignal™ West Femto Maximum Sensitivity Substrate
493 (34095; Thermo Fisher Scientific). Antibodies were stripped in 1:1 (v:v) 10% SDS and 100 mM
494 glycine-HCl (pH 2.5) solution, washed five times, and reblotted with anti-MPK6 antibody
495 (1:8000; Sigma-Aldrich) and anti-MPK3 antibody (1:2500; Sigma-Aldrich). HRP-conjugated
496 anti-rabbit secondary antibody (1:10000; GE Healthcare) was used and signals detected with
497 Western Lightning Plus Electrochemiluminescence (NEL105001EA; PerkinElmer). All blots
498 were imaged in a ChemiDoc XRS+ imaging system (Bio-Rad).
499

500 **Immunoblots**

501 The Arabidopsis seedlings were ground in liquid N_2, resuspended in total protein extraction
502 buffer (25 mM Tris-HCl, pH 7.5, 150 mM NaCl, and Roche cOmplete ULTRA protease
503 inhibitor cocktail, Roche PhosSTO tablet) in a 1:2 (w/v) ratio, and centrifuged at 15,000*g*. The
504 supernatants were mixed with required amount of 4× NuPAGE lithium dodecyl sulphate (LDS)
505 sample buffer (Invitrogen) and 10× NuPAGE sample-reducing agent (Invitrogen), heated at
506 70°C for 10 min, and loaded onto 4-20% Mini-PROTEAN TGX precast gels. The proteins were
507 transferred to nitrocellulose membranes by means of the Trans-Blot® Turbo™ Transfer System
508 (Bio-Rad). For protein detection, the following antibodies were used: monoclonal α-GFP-HRP
509 (1/5,000; Miltenyi Biotech), monoclonal α-tubulin (1/10,000; Sigma-Aldrich), α-BES1
510 (1:4,000; Yin et al., 2002), α-BAK1 (1/5,000; custom-made by Eurogentec). Blots were
511 developed with Western Lightning Plus-ECL, Enhanced Chemiluminescence Substrate
512 (Perkin-Elmer), and imaged with the Bio-Rad ChemiDoc XRS+molecular imager.

513 **TAMRA-Pep1 internalization assay and image analysis**

514 Five-day-old seedlings were dipped into 500 µl of 100 nM TAMRA-Pep1 dissolved in ½MS
515 medium for 10 sec, washed with ½MS liquid medium three times, and kept in 500 µl of ½MS
516 medium over a Parafilm piece in a Petri plate. The epidermal cells of the root meristematic zone
517 were imaged at the indicated time points with a laser scanning confocal microscope SP8X
518 (Leica) equipped with an HC PL APO CS2 40×/1.10 water-corrected objective with 4× digital
519 zoom. The excitation wavelength was 559 nm by white light laser. Emission was detected at
520 570-670 nm by hybrid detectors (Leica). For the image quantification with FIJI
521 (https://imagej.net/software/fiji/), the first images were converted to 8-bit images;
522 subsequently, the entire plasma membranes of individual cells were selected with the brush tool
523 size 10 pixels and the intracellular spaces with the polygon selection tool. The number of the
524 5% highest pixels was obtained for both PM and intracellular space. These values were used to
525 obtain a ratio. Ten epidermal cells from five plants were quantified.

526

527 **AFCS uptake assays and image analysis**

528 The AFCS uptake assay was done as previously described (Irani *et al*, 2014) with modifications.
529 Six-day-old seedlings grown on solid ½MS were transferred to 200 µl of liquid ½MS on a
530 Parafilm piece placed in a Petri plate, humidified with wet laboratory wipes for 10 min. The
531 medium was replaced with ½MS supplemented with 30 µM AFCS for 40 min (pulse).
532 Seedlings were washed six times and chased for 30 min on ½MS followed by imaging.
533 Epidermal cells of the root meristematic zone were imaged with the laser scanning confocal
534 microscope SP8X (Leica) equipped with an HC PL APO CS2 63×/1.20 water-corrected
535 objective with 4× digital zoom. The excitation wavelength was 633 nm by white light laser.
536 Emission was detected at 650-700 nm by hybrid detectors (Leica). For fluorescence signal
537 measurements in vacuoles, stacks of four to six slices of 1.5 µm were obtained. Images were
538 analyzed and signals quantified with the Fiji/ImageJ software. Four to six slices covering the
539 epidermal cell layer were merged by means of maximum projection. The images were
540 processed with Gaussian blur filter (1) and Subtraction Background (100). Rectangular regions
541 of interest were determined omitting over-stained regions, such as the lateral root cap. The
542 signal intensity was quantified in seven to nine seedlings per genotype.

543

544 **Protein production and purification**

545 For GST-tagged protein production, the *E. coli* strain Rosetta2 harboring each of the plasmids
546 pGEX-5×1-PEPR1-CD, pGEX-5×1-PEPR1-Km-CD or *pDEST15-BIK1-Km(KK105AA)* was

547 grown in Luria-Bertani (LB) medium supplemented with carbenicillin (100 µg/ml) at 37˚C until
548 an optical density OD_{600} of 0.6-0.8. Protein production was induced with 1 mM isopropyl β-D-
549 1-thiogalactopyranoside (IPTG) at 16°C overnight, and shaking at 200 rpm. The bacterial
550 culture was pelleted (15 min, 5000*g*) and frozen at -20°C. The cells were resuspended in
551 extraction buffer [50 mM Tris-HCl, pH 8.5, 100 mM NaCl, 1 mM EDTA, 1 mM DTT, protease
552 inhibitor cocktail tablet (cOmplete ULTRA Tablets; Roche), 1 mg/ml lysozyme, 0.4 mM
553 PMSF, 1% Triton X-100] and incubated on ice for 60 min. Resuspended cells were sonicated
554 until the solution became fluid and clear. The lysate was centrifuged (30 min, 12000*g* at 4˚C)
555 and the supernatant was transferred to a new tube. Proteins were purified with Glutathione
556 Sepharose® 4B (GE Healthcare). Glutathione Sepharose slurry (300 µl) was washed twice with
557 binding buffer (50 mM Tris-HCl, pH 8.5, 100 mM NaCl, 1 mM EDTA, and 1 mM DTT) by
558 addition of 5 ml buffer for 1 ml slurry. After washing, the slurry was added to the lysate and
559 incubated for 60 min on an end-to-end rotor at 4˚C. After incubation, slurry was spun down
560 (5 min, 500*g*) and washed twice with 10 ml washing buffer A (50 mM Tris-HCl, pH 8.5,
561 100 mM NaCl, 1 mM EDTA, 1 mM DTT, and 0.1% [v/v] Triton X-100) for 15 min on an end-
562 to-end rotor at 4°C. The slurry was further washed twice with 10 ml binding buffer (50 mM
563 Tris-HCl, pH 8.5, 100 mM NaCl, 1 mM EDTA, 1 mM DTT) for 15 min on an end-to-end rotor
564 at 4˚C. For elution, the slurry was incubated for 10 min at room temperature on an end-to-end
565 rotor with 500 µl elution buffer (50 mM Tris-HCl, pH 8.5, 100 mM NaCl, 1 mM EDTA, 1 mM
566 DTT, 20 mM freshly prepared gluthatione, pH 8.0). The elution was repeated three times and
567 the three eluates were pooled and concentrated with Amicon® Ultra 30K (Millipore) until
568 500 µl was obtained.

569 For His6-MBP-tagged proteins, *E. coli* strain Rosetta2 harboring the plasmid *pOPNIM-*
570 *BAK1-CD* and *pOPNIM-BAK1-Km-CD* were grown in LB medium supplemented with
571 100 µg/ml carbenicillin at 37˚C until OD_{600} = 0.6-0.8. Protein production was induced with
572 1 mM of IPTG at 16˚C overnight, with shaking at 200 rpm. The bacterial culture was pelleted
573 (15 min, 5000*g*) and frozen at -20˚C. The cells were resuspended in extraction buffer [20 mM
574 Tris-HCl, pH 8.5, 200 mM NaCl, 1 mM EDTA, 1 mM DTT, protease inhibitor cocktail tablet
575 (cOmplete ULTRA Tablets; Roche), 1 mg/ml lysozyme, 0.4 mM PMSF] and incubated on ice
576 for 60 min. Resuspended cells were sonicated until the solution became fluid and clear. The
577 lysate was centrifuged (30 min, 12000*g* at 4˚C) and the supernatant was transferred to a new
578 tube. Proteins were purified with mylose resin (NEB). Amylose slurry was washed three times
579 with wash buffer (20 mM Tris-HCl pH 8.5, 200 mM NaCl, 1 mM EDTA, and 1 mM DTT) and
580 then incubated with the lysate for 60 min on an end-to-end rotor at 4˚C. After incubation, the

581 slurry was spun down (5 min, 500*g*) and washed three times with 10 ml of wash buffer for
582 15 min on an end-to-end rotor at 4˚C. For elution, the amylose slurry was incubated for 10 min
583 at room temperature on an end-to-end rotor with 1 ml elution buffer (20 mM Tris-HCl pH 8.5,
584 200 mM NaCl, 1 mM EDTA, 1 mM DTT, and 10 mM maltose). Elution was repeated three
585 times and the three eluates were pooled and concentrated with Amicon® Ultra 30K (Millipore)
586 until 500 µl was obtained.
587
588 ***In vitro* kinase assay and in-gel trypsin digestion for mass spectrometry (MS)**
589 The *in vitro* kinase assay was carried out by mixing either GST-PEPR1-CD or GST-PEPR1-
590 Km-CD with His6-MBP-BAK1-CD; all the combinations, including the proteins alone, were
591 tested for autophosphorylation. CDs were mixed with 5 µl of [γ-^{32}P] ATP (1 µCi/µl) and the
592 kinase assay buffer (50 mM Tris-HCl, pH 7.5, 100 mM NaCl, 10 mM $MgCl_2$, and 10 µM ATP)
593 was added in 30 µl final volume. The reaction was incubated for 1 h at 25°C and stopped by
594 addition of 10 µl loading buffer 4× [NuPAGE® LDS Sample Buffer (4×)] and 5 µl of 10×
595 reduction buffer [NuPAGE® Sample Reducing Agent (10×)]. Samples were loaded on 4-20%
596 precast SDS-PAGE gels (Bio-Rad). The gels were stained with Bio-Safe Coomassie Brilliant
597 Blue (CBB) (Bio-Rad), dried between cellophane plastic sheets, and [γ-^{32}P] was detected by
598 autoradiography. To examine the phosphorylation sites by MS, an *in vitro* kinase experiment
599 with non-radioactive ATP was conducted after the previously described steps. After the kinase
600 reaction had ended, the samples were segregated by SDS-PAGE and then stained with CBB.
601 Thereafter, in-gel trypsin digestion was carried out, as outlined previously. The resulting
602 digested peptides were purified with OMIX C18 Pipette Tips (Agilent Technologies) and
603 subsequently subjected to a liquid chromatography-tandem MS (MS/MS).
604
605 **Detection of protein phosphorylation in the *Nicotiana benthamiana* leaf epidermis**
606 Agrobacteria containing *P19*, *p35S-PEPR1-Km-GFP* or *p35S-BAK1-mCherry* were co-
607 infiltrated into *Nicotiana benthamiana* leaves with the combination shown in the figure. After
608 60 hours, leaves were treated with water or 500 nM Pep1 for 15 min by injection before
609 harvesting. Four biologically replicated samples per experimental group were ground with
610 liquid nitrogen. Total protein was extracted from 5 mL of compacted plant powder using
611 extraction buffer [50 mM Tris-HCl pH7.5, 150 mM NaCl, 1 mM EDTA, 1% NP-40, 5%
612 glycerol, protease inhibitor cocktail (Roche) and PhosSTOP (Roche)]. Immunoprecipitation
613 was performed with GFP-Trap magnetic agarose (ChromoTek) followed by 3 washes with wash
614 buffer (50 mM Tris-HCl pH7.5, 150 mM NaCl, 1 mM EDTA and 1% NP-40) and 1 wash with

615 50 mM TEAB pH8.0 (Thermo Fischer). Protein was eluted on beads using 0.5 µg trypsin, and
616 then alkylated of cysteine residues using 15 mM tris(carboxyethyl)phosphine (TCEP, Pierce)
617 and 30 mM iodoacetamide (Sigma-Aldrich). The peptides were completely digested by
618 incubation with 0.5 µg trypsin for 16 hours and desalting with OMIX C18 pipette tips (Agilent
619 Technologies). The LC-MS/MS analyses were carried out as described previously (Vu *et al.*
620 2021). Peptide searches were performed using MaxQuant (version 2.1.4.0) on a high
621 performance computer (HPC-UGent) against a database containing all *Nicotiana benthamiana*
622 protein sequences from UniProt (Proteome ID: UP000084051) and the *Arabidopsis thaliana*
623 protein sequences of PEPR1-Km-GFP and BAK1-mCherry.
624

625 **Database searching and data analysis**

626 MS/MS spectra were searched with the BL21(DE3) proteome database and the sequences of
627 GST-PEPR1-CD, GST-PEPR1-CD-kinase dead, HIS6-MBP-BAK1-CD, and HIS6-MBP-
628 BAK1-Km-CD with the MaxQuant software (version 1.6.17.0) by means of the UseGalaxy.be
629 server. MaxQuant settings can be found in Dataset EV1. The 'Phospho (STY).txt' output file
630 generated by the MaxQuant search was loaded into the Perseus software (version 1.6.7.0) for
631 analysis. All the data were selected first by a localization probe cut-off of >0.75. The Log2-
632 transformed phosphosite intensities were used for further analysis. The 'proteinGroups.txt' file
633 was also loaded into the Perseus software (version 1.6.7.0) for analysis. The label-free
634 quantification (LFQ) intensities were loaded and transformed by Log2 for further analysis.
635

636 **CCV Purification**

637 Seven-day-old *pRPS5A-PEPR1-GFP/pepr1pepr2* seedlings were grown in ½MS. A sample of
638 30 g was ground at 4°C and fractionated to purify CCVs as described previously (Mosesso *et*
639 *al*, 2019). Samples collected during the purification and the final CCV fraction were analyzed
640 by immunoblot analysis with antibodies against organelles and/or cellular compartments. The
641 antibodies used were: HRP-coupled monoclonal α-GFP (1:2,500; Miltenyi Biotech), α-CHC
642 (1:5,000; Santa Cruz Biotechnologies), α-H^+ ATPase (1:5,000; Agrisera), α-V-ATPase
643 (1:5,000; Agrisera), and α-BiP (1:2,000; Agrisera).
644

645 **RT-qPCR**

646 Total RNA was extracted from approximately 100 mg of 5-day-old seedlings with the RNeasy
647 kit (Qiagen). cDNA was synthesized from 1000 ng of RNA with the qScript cDNA Supermix
648 (Quantabio). The resulting cDNA was diluted to 1:5 with nuclease-free water. RT-qPCRs were

run with SYBR green I Master kit (Roche) on a LightCycler 480 (Roche). Expression was normalized to that of *ACTIN2* and *GAPDH* genes. The cycling conditions were as follows: preincubation at 95°C for 10 min; 45 amplification cycles at 95°C for 10 s, 60°C for 15 s, and 72°C for 15 s; melting curve at 95°C for 1 s, and 65°C for 1 s, followed by cooling at 40°C for 10 s. The integrity of the PCR amplicon was confirmed by melting curve analyses. The primers used are listed in Table EV1

Quantification and statistical analysis

All statistical analyses were carried out in GraphPad Prism 9. Statistically significant differences were determined by one-way or two-way Analysis of Variance (ANOVA) test.

Data availability

No data were deposited in external repositories. Data used for quantifications as well as full Western blots can be found in the source data file. All material will be made available upon request to the corresponding author (eugenia.russinova@psb.vib-ugent.be).

SUPPLEMENTAL INFORMATION

Supplemental information is available online

FUNDING

This work was supported by special research funding from the Flemish Government and funding from the Student Program-Graduate Studies Plan Program from the Coordination for the Improvement of Higher Education Personnel (Brazil) for a for a joint doctorate fellowship at Ghent University and University of São Paulo to FAO-M; the European Union's Horizon 2020 research and innovation program under the Marie Sklodowska-Curie grant agreement (No 101023079 'ENDOLOGISTIC') to SY; PEW Latin American Fellows Program to FAO-M, the National Science Foundation (NSF) (MCB-1906060) to PH, and NSF (IOS-2049642) to LS, the China Scholarship Council for a predoctoral fellowship (201706350153) and a UGent BOF doctoral mandate (01CD7122) to XX, and the Research Foundation-Flanders (G003720N) to ER. The computational resources (Stevin Supercomputer Infrastructure) and services used in this work were provided by the VSC (Flemish Supercomputer Center), funded by Ghent University, FWO and the Flemish Government – department EWI.

AUTHOR CONTRIBUTIONS

L.A.N.C., F.A.O.-.M. and E.R. initiated and designed the experiments. L.A.N.C. did most of the work. X. X., S.-L. Y. and I.D.S. identified the *in vitro* / *in vivo* phosphorylation sites. S. Y. did phenotypic analysis. I.Y. performed some MAPK and ROS assays. I. D.S., P.H., L.S., and E.R. provided supervision, funding and analyzed the data. L.A.N.C. and E.R. wrote the manuscript and all authors revised it.

ACKNOWLEDGEMENTS

We thank Yanhai Yin for providing the α-BES1 antibody, Cyril Zipfel for published materials, Guilherme Perreira de Oliveira and Simone Di Rubbo for technical help, Daniel Scherer de Moura and Daniel V. Savatin for constructive discussions, and Martine De Cock for help in preparing the manuscript.

DISCLOSURE AND COMPETING INTERESTS STATEMENT

The authors declare that they have no conflict of interest.

REFERENCES

Bartels S, Boller T (2015) Quo vadis, Pep? Plant elicitor peptides at the crossroads of immunity, stress, and development. *J Exp Bot* 66: 5183-5193

Bartels S, Lori M, Mbengue M, van Verk M, Klauser D, Hander T, Böni R, Robatzek S, Boller T (2013) The family of Peps and their precursors in *Arabidopsis*: differential expression and localization but similar induction of pattern-triggered immune responses. *J Exp Bot* 64: 5309-5321

Beck M, Zhou J, Faulkner C, MacLean D, Robatzek S (2012) Spatio-temporal cellular dynamics of the *Arabidopsis* flagellin receptor reveal activation status-dependent endosomal sorting *Plant Cell* 24: 4205-4219

Bender KW, Couto D, Kadota Y, Macho AP, Sklenar J, Derbyshire P, Bjornson M, DeFalco TA, Petriello A, Font Farre M *et al* (2021) Activation loop phosphorylation of a non-RD receptor kinase initiates plant innate immune signaling. *Proc Natl Acad Sci USA* 118: e2108242118

Berrow NS, Alderton D, Sainsbury S, Nettleship J, Assenberg R, Rahman N, Stuart DI, Owens RJ (2007) A versatile ligation-independent cloning method suitable for high-throughput expression screening applications. *Nucleic Acids Res* 35: e45

Bücherl CA, van Esse GW, Kruis A, Luchtenberg J, Westphal AH, Aker J, van Hoek A, Albrecht C, Borst JW, de Vries SC (2013) Visualization of BRI1 and BAK1(SERK3)

717 membrane receptor heterooligomers during brassinosteroid signaling *Plant Physiol* 162:
718 1911-1925
719 Chinchilla D, Zipfel C, Robatzek S, Kemmerling B, Nürnberger T, Jones JDG, Felix G,
720 Boller T (2007) A flagellin-induced complex of the receptor FLS2 and BAK1 initiates
721 plant defence. *Nature* 448: 497-500
722 Choi J, Tanaka K, Cao Y, Qi Y, Qiu J, Liang Y, Lee SY, Stacey G (2014) Identification of a
723 plant receptor for extracellular ATP. *Science* 343: 290-294
724 Claus LAN, Savatin DV, Russinova E (2018) The crossroads of receptor-mediated signaling
725 and endocytosis in plants. *J Integr Plant Biol* 60: 827-840
726 Clough SJ, Bent AF (1998) Floral dip: a simplified method for *Agrobacterium*-mediated
727 transformation of *Arabidopsis thaliana*. *Plant J* 16: 735-743
728 Du J, Gao Y, Zhan Y, Zhang S, Wu Y, Xiao Y, Zou B, He K, Gou X, Li G *et al.* (2016)
729 Nucleocytoplasmic trafficking is essential for BAK1- and BKK1-mediated cell-death
730 control. *Plant J* 85: 520-531
731 Dubeaux G, Neveu J, Zelazny E, Vert G (2018) Metal sensing by the IRT1 transporter-
732 receptor orchestrates its own degradation and plant metal nutrition. *Mol Cell* 69: 953-964
733 Dubeaux G, Vert G (2017) Zooming into plant ubiquitin-mediated endocytosis. *Curr Opin*
734 *Plant Biol* 40: 56-62
735 Ekanayake G, Smith JM, Jones KB, Stiers HM, Robinson SJ, LaMontagne ED, Kostos PH,
736 Cornish PV, Bednarek SY, Heese A (2021) DYNAMIN-RELATED PROTEIN DRP1A
737 functions with DRP2B in plant growth, flg22-immune responses, and endocytosis. *Plant*
738 *Physiol* 185: 1986-2002
739 Erwig J, Ghareeb H, Kopischke M, Hacke R, Matei A, Petutschnig E, Lipka V (2017) Chitin-
740 induced and CHITIN ELICITOR RECEPTOR KINASE1 (CERK1) phosphorylation-
741 dependent endocytosis of *Arabidopsis thaliana* LYSIN MOTIF-CONTAINING
742 RECEPTOR-LIKE KINASE5 (LYK5). *New Phytol* 215: 382-396
743 Fan M, Wang M, Bai M-Y (2016) Diverse roles of SERK family genes in plant growth,
744 development and defense response. *Sci China Life Sci* 59: 889-896
745 Geldner N, Anders N, Wolters H, Keicher J, Kornberger W, Muller P, Delbarre A, Ueda T,
746 Nakano A, Jürgens G (2003) The *Arabidopsis* GNOM ARF-GEF mediates endosomal
747 recycling, auxin transport, and auxin-dependent plant growth. *Cell* 112: 219-230
748 Hammond JW, Blasius TL, Soppina V, Cai D, Verhey KJ (2010) Autoinhibition of the
749 kinesin-2 motor KIF17 via dual intramolecular mechanisms. *J Cell Biol* 189: 1013-1025

750 Hou S, Liu Z, Shen H, Wu D (2019) Damage-associated molecular pattern-triggered
751 immunity in plants. *Front Plant Sci* 10: 646
752 Huffaker A, Dafoe NJ, Schmelz EA (2011) ZmPep1, an ortholog of Arabidopsis elicitor
753 peptide 1, regulates maize innate immunity and enhances disease resistance. *Plant*
754 *Physiol* 155: 1325-1338
755 Huffaker A, Pearce G, Veyrat N, Erb M, Turlings TCJ, Sartor R, Shen Z, Briggs SP, Vaughan
756 MM, Alborn HT *et al* (2013) Plant elicitor peptides are conserved signals regulating
757 direct and indirect antiherbivore defense. *Proc Natl Acad Sci USA* 110: 5707-5712
758 Hurst CH, Turnbull D, Myles SM, Leslie K, Keinath NF, Hemsley PA (2018) Variable effects
759 of C-terminal fusions on FLS2 function: not all epitope tags are created equal. *Plant*
760 *Physiol* 177: 522-531
761 Irani NG, Di Rubbo S, Mylle E, Van den Begin J, Schneider-Pizoń J, Hniliková J, Šiša M,
762 Buyst D, Vilarrasa-Blasi J, Szatmári A-M *et al* (2012) Fluorescent castasterone reveals
763 BRI1 signaling from the plasma membrane. *Nat Chem Biol* 8: 583-589
764 Irani NG, Di Rubbo S, Russinova E (2014) In vivo imaging of brassinosteroid endocytosis in
765 Arabidopsis. *Methods Mol Biol* 1209: 107-117
766 Jaillais Y, Vert G (2016) Brassinosteroid signaling and BRI1 dynamics went underground.
767 *Curr Opin Plant Biol* 33: 92-100
768 Kim SY, Xu Z-Y, Song K, Kim DH, Kang H, Reichardt I, Sohn EJ, Friml J, Juergens G,
769 Hwang I (2013) Adaptor protein complex 2–mediated endocytosis is crucial for male
770 reproductive organ development in *Arabidopsis*. *Plant Cell* 25: 2970-2985
771 Krol E, Mentzel T, Chinchilla D, Boller T, Felix G, Kemmerling B, Postel S, Arents M,
772 Jeworutzki E, Al-Rasheid KAS *et al* (2010) Perception of the *Arabidopsis* danger signal
773 peptide 1 involves the pattern recognition receptor *At*PEPR1 and its close homologue
774 *At*PEPR2. *J Biol Chem* 285: 13471-13479
775 Li B, Ferreira MA, Huang M, Camargos LF, Yu X, Teixeira RM, Carpinetti PA, Mendes GC,
776 Gouveia-Mageste BC, Liu C *et al* (2019) The receptor-like kinase NIK1 targets
777 FLS2/BAK1 immune complex and inversely modulates antiviral and antibacterial
778 immunity. *Nat Commun* 10: 4996
779 Lin W, Li B, Lu D, Chen S, Zhu N, He P, Shan L (2014) Tyrosine phosphorylation of protein
780 kinase complex BAK1/BIK1 mediates Arabidopsis innate immunity. *Proc Natl Acad Sci*
781 *USA* 111: 3632-3637
782 Liu D, Kumar R, Claus LAN, Johnson AJ, Siao W, Vanhoutte I, Wang P, Bender KW,
783 Yperman K, Martins S *et al* (2020) Endocytosis of BRASSINOSTEROID

784 INSENSITIVE1 is partly driven by a canonical Tyr-based motif. *Plant Cell* 32: 3598-
785 3612
786 Liu J, Chen S, Chen L, Zhou Q, Wang M, Feng D, Li J-F, Wang J, Wang H-B, Liu B (2017)
787 BIK1 cooperates with BAK1 to regulate constitutive immunity and cell death in
788 *Arabidopsis*. *J Integr Plant Biol* 59: 234-239
789 Liu Y, Huang X, Li M, He P, Zhang Y (2016) Loss-of-function of *Arabidopsis* receptor-like
790 kinase BIR1 activates cell death and defense responses mediated by BAK1 and SOBIR1.
791 *New Phytol* 212: 637-645
792 Liu Z, Wu Y, Yang F, Zhang Y, Chen S, Xie Q, Tian X, Zhou J-M (2013) BIK1 interacts
793 with PEPRs to mediate ethylene-induced immunity. *Proc Natl Acad Sci USA* 110: 6205-
794 6210
795 Lozano-Durán R, Macho AP, Boutrot F, Segonzac C, Somssich IE, Zipfel C (2013) The
796 transcriptional regulator BZR1 mediates trade-off between plant innate immunity and
797 growth. *eLife* 2: e00983
798 Lu D, Lin W, Gao X, Wu S, Cheng C, Avila J, Heese A, Devarenne TP, He P, Shan L (2011)
799 Direct ubiquitination of pattern recognition receptor FLS2 attenuates plant innate
800 immunity. *Science* 332: 1439-1442
801 Lu D, Wu S, Gao X, Zhang Y, Shan L, He P (2010) A receptor-like cytoplasmic kinase,
802 BIK1, associates with a flagellin receptor complex to initiate plant innate immunity. *Proc*
803 *Natl Acad Sci USA* 107: 496-501
804 Ma X, Claus LAN, Leslie ME, Tao K, Wu Z, Liu J, Yu X, Li B, Zhou J, Savatin DV *et al*
805 (2020) Ligand-induced monoubiquitination of BIK1 regulates plant immunity. *Nature*
806 581: 199-203
807 Martins S, Dohmann EMN, Cayrel A, Johnson A, Fischer W, Pojer F, Satiat-Jeunemaître B,
808 Jaillais Y, Chory J, Geldner N *et al* (2015) Internalization and vacuolar targeting of the
809 brassinosteroid hormone receptor BRI1 are regulated by ubiquitination. *Nat Commun* 6:
810 6151
811 Mbengue M, Bourdais G, Gervasi F, Beck M, Zhou J, Spallek T, Bartels S, Boller T, Ueda T,
812 Kuhn H *et al* (2016) Clathrin-dependent endocytosis is required for immunity mediated
813 by pattern recognition receptor kinases. *Proc Natl Acad Sci USA* 113: 11034-11039
814 Meng X, Chen X, Mang H, Liu C, Yu X, Gao X, Torii Keiko U, He P, Shan L (2015)
815 Differential function of *Arabidopsis* SERK family receptor-like kinases in stomatal
816 patterning. *Curr Biol* 25: 2361-2372

817 Mosesso N, Bläske T, Nagel M-K, Laumann M, Isono E (2019) Preparation of clathrin-coated
818 vesicles from *Arabidopsis thaliana* seedlings. *Front Plant Sci* 9: 1972
819 Mühlenbeck H, Tsutsui Y, Lemmon MA, Bender KW, Zipfel C (2024) Allosteric activation
820 of the co-receptor BAK1 by the EFR receptor kinase initiates immune signaling. *eLife* 12:
821 RP92110
822 Ntoukakis V, Schwessinger B, Segonzac C, Zipfel C (2011) Cautionary notes on the use of C-
823 terminal BAK1 fusion proteins for functional studies. *Plant Cell* 23: 3871-3878
824 Ortiz-Morea FA, Savatin DV, Dejonghe W, Kumar R, Luo Y, Adamowski M, Van den Begin
825 J, Dressano K, Pereira de Oliveira G, Zhao X *et al* (2016) Danger-associated peptide
826 signaling in *Arabidopsis* requires clathrin. *Proc Natl Acad Sci USA* 113: 11028-11033
827 Pavlos NJ, Friedman PA (2017) GPCR signaling and trafficking: The long and short of it.
828 *Trends Endocrinol Metab* 28: 213-226
829 Pei D, Hua D, Deng J, Wang Z, Song C, Wang Y, Wang Y, Qi J, Kollist H, Yang S *et al*
830 (2022) Phosphorylation of the plasma membrane H^+-ATPase AHA2 by BAK1 is required
831 for ABA-induced stomatal closure in Arabidopsis. *Plant Cell* 34: 2708-2729
832 Perraki A, DeFalco TA, Derbyshire P, Avila J, Séré D, Sklenar J, Qi X, Stransfeld L,
833 Schwessinger B, Kadota Y *et al* (2018) Phosphocode-dependent functional dichotomy of
834 a common co-receptor in plant signalling. *Nature* 561: 248-252
835 Robatzek S, Chinchilla D, Boller T (2006) Ligand-induced endocytosis of the pattern
836 recognition receptor FLS2 in *Arabidopsis*. *Genes Dev* 20: 537-542
837 Russinova E, Borst J-W, Kwaaitaal M, Caño-Delgado A, Yin Y, Chory J, de Vries SC (2004)
838 Heterodimerization and endocytosis of Arabidopsis brassinosteroid receptors BRI1 and
839 AtSERK3 (BAK1). *Plant Cell* 16: 3216-3229
840 Schulze B, Mentzel T, Jehle AK, Mueller K, Beeler S, Boller T, Felix G, Chinchilla D (2010)
841 Rapid heteromerization and phosphorylation of ligand-activated plant transmembrane
842 receptors and their associated kinase BAK1. *J Biol Chem* 285: 9444-9451
843 Schwessinger B, Roux M, Kadota Y, Ntoukakis V, Sklenar J, Jones A, Zipfel C (2011)
844 Phosphorylation-dependent differential regulation of plant growth, cell death, and innate
845 immunity by the regulatory receptor-like kinase BAK1. *PLoS Genet* 7: e1002046
846 Sigismund S, Confalonieri S, Ciliberto A, Polo S, Scita G, Di Fiore PP (2012) Endocytosis
847 and signaling: cell logistics shape the eukaryotic cell plan. *Physiol Rev* 92: 273-366
848 Song L, Shi Q-M, Yang X-H, Xu Z-H, Xue H-W (2009) Membrane steroid-binding protein 1
849 (MSBP1) negatively regulates brassinosteroid signaling by enhancing the endocytosis of
850 BAK1. *Cell Res* 19: 864-876

851 Takano J, Tanaka M, Toyoda A, Miwa K, Kasai K, Fuji K, Onouchi H, Naito S, Fujiwara T
852 (2010) Polar localization and degradation of *Arabidopsis* boron transporters through
853 distinct trafficking pathways. *Proc Natl Acad Sci USA* 107: 5220-5225
854 Tang J, Han Z, Sun Y, Zhang H, Gong X, Chai J (2015) Structural basis for recognition of an
855 endogenous peptide by the plant receptor kinase PEPR1. *Cell Res* 25: 110-120
856 Tunc-Ozdemir M, Li B, Jaiswal DK, Urano D, Jones AM, Torres MP (2017) Predicted
857 functional implications of phosphorylation of regulator of G protein signaling protein in
858 plants. *Front Plant Sci* 8: 1456
859 Vu LD, Xu X, Zhu T, Pan L, van Zanten M, de Jong D, Wang Y, Vanremoortele T, Locke
860 AM, van de Cotte B et al. (2021) The membrane-localized protein kinase
861 MAP4K4/TOT3 regulates thermomorphogenesis. *Nat Commun* 12: 2842.
862 Wang S, Yoshinari A, Shimada T, Hara-Nishimura I, Mitani-Ueno N, Feng Ma J, Naito S,
863 Takano J (2017) Polar localization of the NIP5;1 boric acid channel is maintained by
864 endocytosis and facilitates boron transport in Arabidopsis roots. *Plant Cell* 29: 824-842
865 Wang X, Kota U, He K, Blackburn K, Li J, Goshe MB, Huber SC, Clouse SD (2008)
866 Sequential transphosphorylation of the BRI1/BAK1 receptor kinase complex impacts
867 early events in brassinosteroid signaling. *Dev Cell* 15: 220-235
868 Wang Y, Li Z, Liu D, Xu J, Wei X, Yan L, Yang C, Lou Z, Shui W (2014) Assessment of
869 BAK1 activity in different plant receptor-like kinase complexes by quantitative profiling
870 of phosphorylation patterns. *J Proteomics* 108: 484-493
871 Wang Z-Y, Seto H, Fujioka S, Yoshida S, Chory J (2001) BRI1 is a critical component of a
872 plasma-membrane receptor for plant steroids. *Nature* 410: 380–383
873 Willems P, Sterck L, Dard A, Huang J, De Smet I, Gevaert K, Van Breusegem F (2024) The
874 Plant PTM Viewer 2.0: in-depth exploration of plant protein modification landscapes. *J*
875 *Exp Bot* 75: 4611-4624
876 Wiśniewska J, Xu J, Seifertová D, Brewer PB, Růžička K, Blilou I, Rouquié D, Benková E,
877 Scheres B, Friml J (2006) Polar PIN localization directs auxin flow in plants. *Science*
878 312: 883-883
879 Wu D, Liu Y, Xu F, Zhang Y (2018) Differential requirement of BAK1 C-terminal tail in
880 development and immunity. *J Integr Plant Biol* 60: 270-275
881 Yamada K, Yamashita-Yamada M, Hirase T, Fujiwara T, Tsuda K, Hiruma K, Saijo Y (2016)
882 Danger peptide receptor signaling in plants ensures basal immunity upon pathogen-
883 induced depletion of BAK1. *EMBO J* 35: 46-61

884 Yamaguchi Y, Huffaker A (2011) Endogenous peptide elicitors in higher plants. *Curr Opin*
885 *Plant Biol* 14: 351-357
886 Yamaguchi Y, Huffaker A, Bryan AC, Tax FE, Ryan CA (2010) PEPR2 is a second receptor
887 for the Pep1 and Pep2 peptides and contributes to defense responses in *Arabidopsis.*
888 *Plant Cell* 22: 508-522
889 Yin Y, Wang Z-Y, Mora-Garcia S, Li J, Yoshida S, Asami T, Chory J (2002) BES1
890 accumulates in the nucleus in response to brassinosteroids to regulate gene expression
891 and promote stem elongation. *Cell* 109: 181-191
892 Yu X, Xie Y, Luo D, Liu H, de Oliveira MVV, Qi P, Kim S-I, Ortiz-Morea FA, Liu J, Chen
893 Y *et al* (2023) A phospho-switch constrains BTL2-mediated phytocytokine signaling in
894 plant immunity. *Cell* 186: 2329-2344
895 Zhang J, Li W, Xiang T, Liu Z, Laluk K, Ding X, Zou Y, Gao M, Zhang X, Chen S *et al*
896 (2010) Receptor-like cytoplasmic kinases integrate signaling from multiple plant immune
897 receptors and are targeted by a *Pseudomonas syringae* effector. *Cell Host Microbe* 7:
898 290-301
899 Zhou J, Liu D, Wang P, Ma X, Lin W, Chen S, Mishev K, Lu D, Kumar R, Vanhoutte I *et al*
900 (2018) Regulation of *Arabidopsis* brassinosteroid receptor BRI1 endocytosis and
901 degradation by plant U-box PUB12/PUB13-mediated ubiquitination. *Proc Natl Acad Sci*
902 *USA* 115: E1906-E1915
903

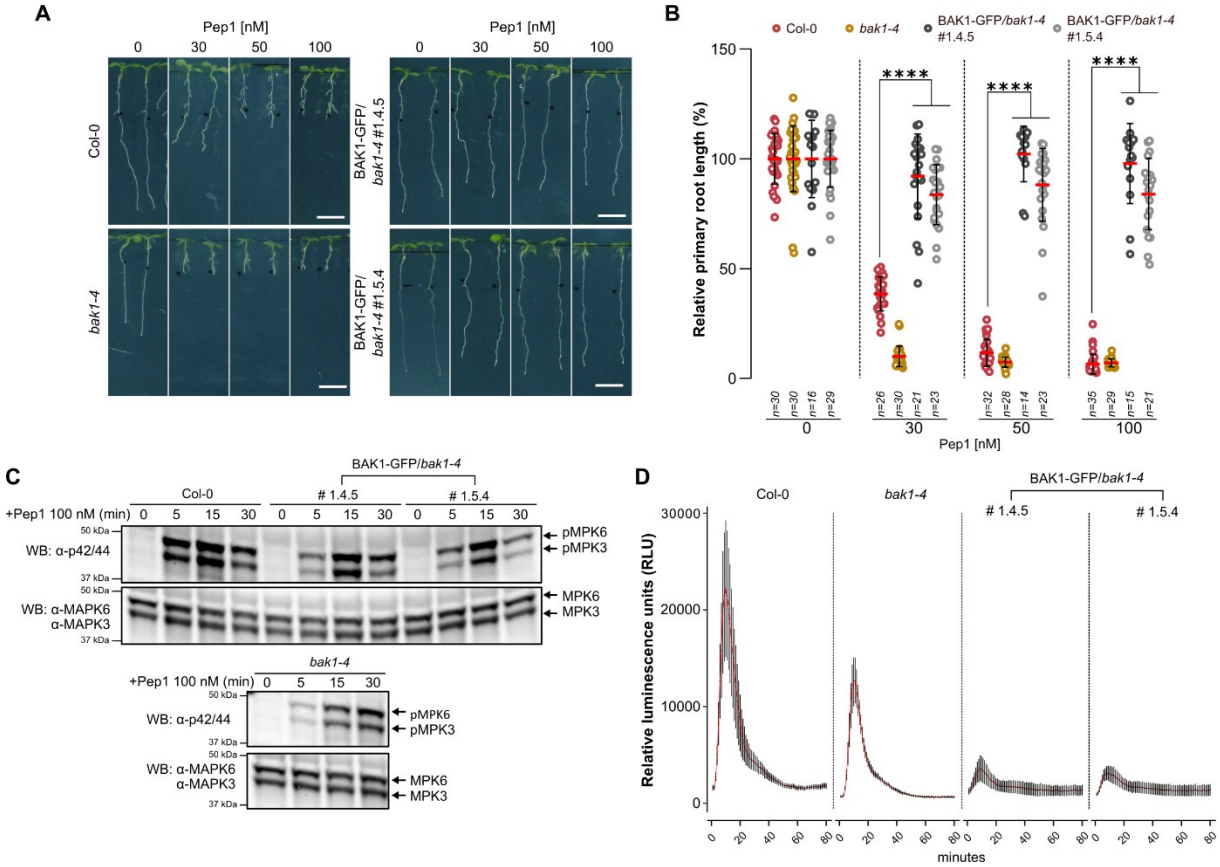

Figure 1. C-terminally tagged BAK1-GFP is not fully functional in Pep1-induced immune responses.

(A) Representative images of root growth inhibition caused by different Pep1 concentrations. Seedlings of wild-type Col-0, *bak1-4*, and two independent *pBAK1-BAK1-GFP*/*bak1-4* transgenic lines (#1.4.5 and #1.5.4) were grown for 4 days on ½MS agar medium and transferred to ½MS agar medium supplemented with different concentrations of Pep1 or water (mock) for a further 3 days. Scale bars, 10 mm.

(B) Primary root length of seedlings in **(A)** presented as relative to the mock-treated control for each genotype. Individual measurements, average, and SD are represented by dots, red lines, and whiskers, respectively. Two-way ANOVA followed by Tukey's test was used to determine significant differences.****$P<0.0001$; *n*, number of seedlings analyzed.

(C) MAPK activation assay of seven-day-old seedlings in **(A)** treated with 100 nM Pep1 for the indicated time points. Phosphorylated MPK3 (pMPK3) and MPK6 (pMPK6) were detected by Western Blotting (WB) with α-p42/44 antibody (top). Protein loading is shown by total MPK3 and MPK6 detected with α-MPK3 and α-MPK6 antibodies (bottom).

(D) Pep1-induced reactive oxygen species (ROS) production. Eight leaf discs from four 5-week-old plants in (A) treated with 100 nM of Pep1. ROS production measured as RLU was detected at the indicated time points. Red lines indicate means ± SD.

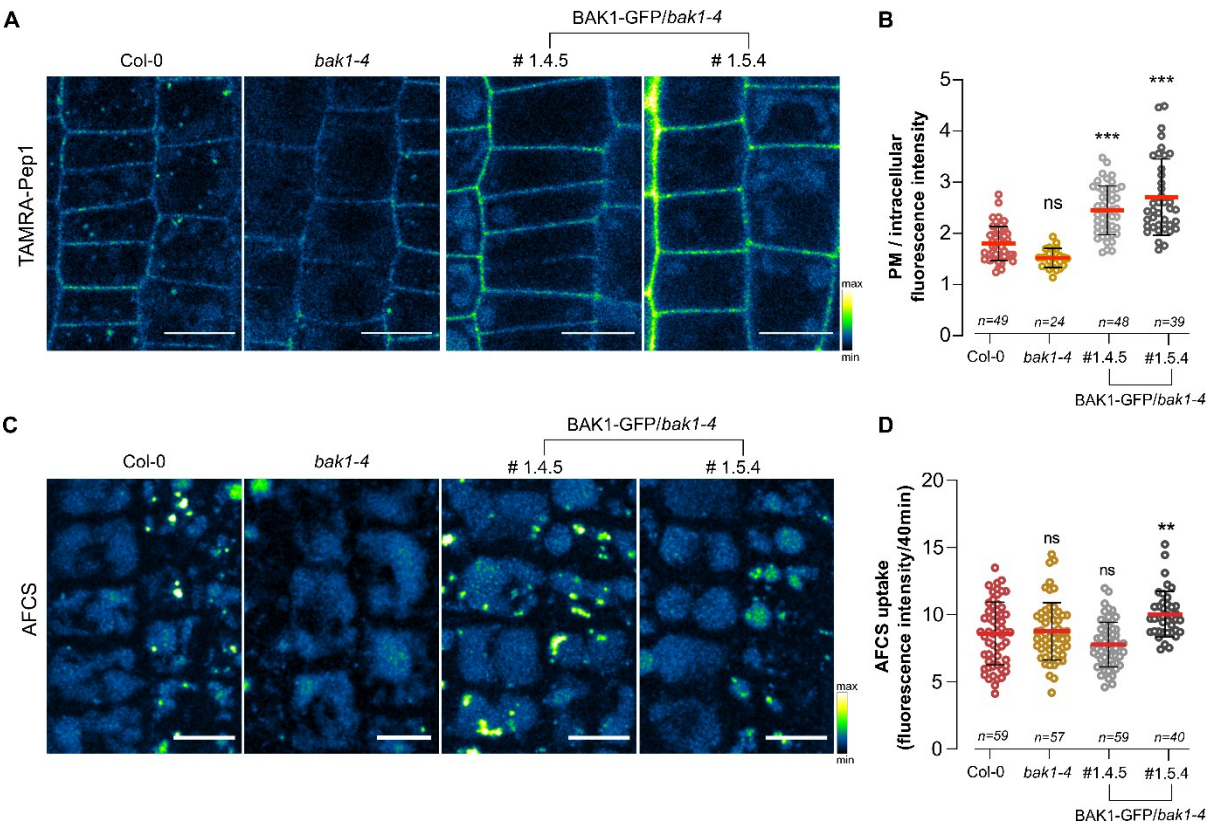

Figure 2. Pep1-triggered PEPR1 endocytosis requires functional BAK1.

(A, C) Representative images of TAMRA-Pep1 **(A)** and AFCS **(C)** root uptake visualized by color-based fluorescence intensity coding. Five-day-old seedlings of wild-type Col-0, *bak1-4*, and two independent *pBAK1-BAK1-GFP*/*bak1-4* transgenic lines were treated with 100 nM TAMRA-Pep1 for 10 s (pulse) and with 40 µM AFCS for 20 min (pulse), respectively, and imaged after 40 min (chase). Epidermal cells of root meristematic zone were imaged. Scale bars, 10 µm.

(B, D) Fluorescence intensity measurements of plasma membrane (PM) vs intracellular compartments of the **(B)** TAMRA-Pep1 uptake in **(A)** and **(D)** the AFCS uptake after 40 min chase in **(C)**. Individual measurements, average, and SD are represented by dots, red line, and whiskers, respectively. One-way ANOVA followed by Tukey's test was used to determine significant differences.***$P<0.001$, **$P<0.01$; *n*, number of cell analyzed; ns, not significant.

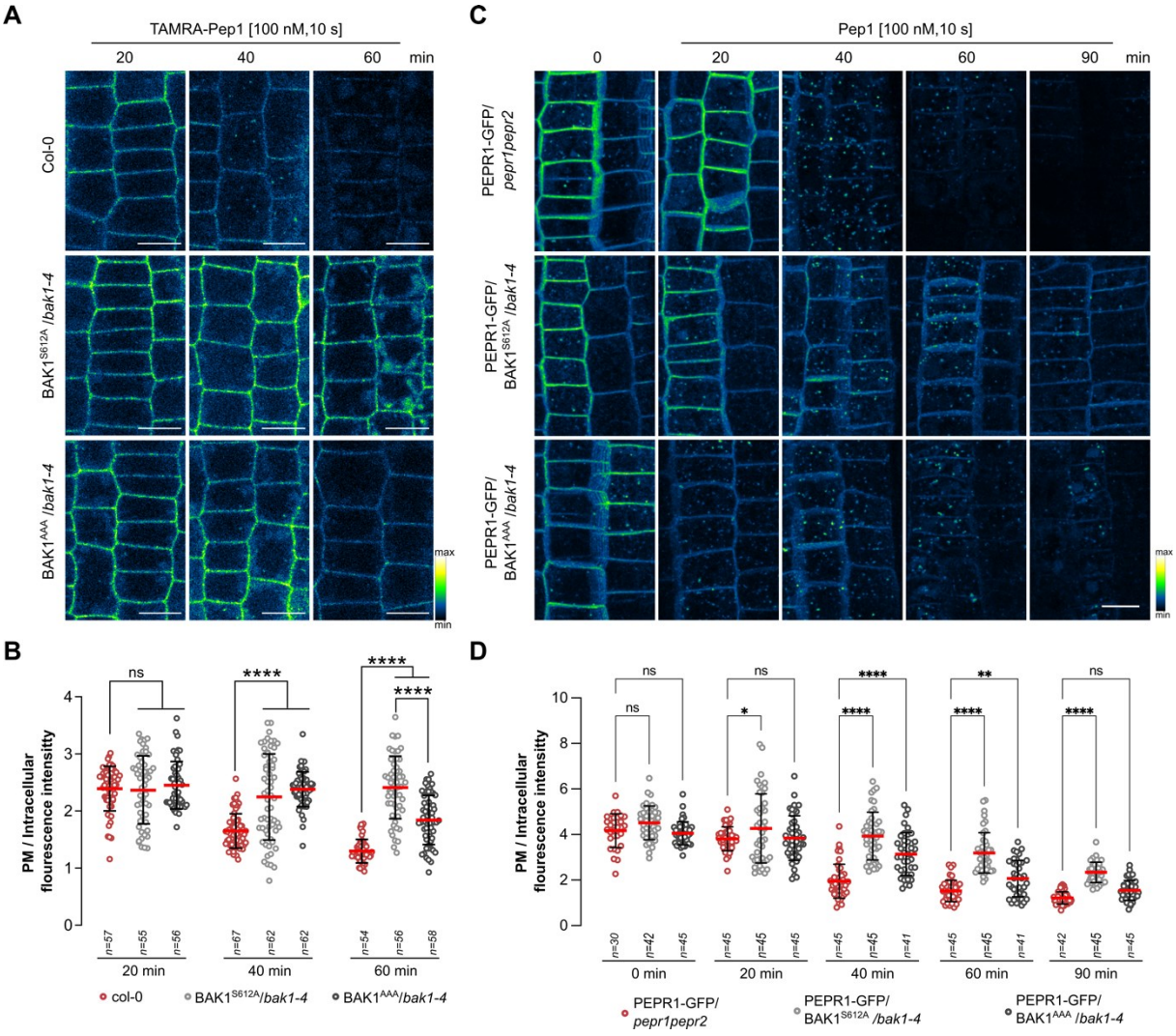

Figure 3. The BAK1 phosphorylation essential for flagellin-induced signaling influences PEPR1 endocytosis.

(A) Representative images of TAMRA-Pep1 root uptake visualized by color-based fluorescence intensity coding. Five-day-old wild-type Col-0, *pBAK1-BAK1^{S612A}/bak1-4* and *pBAK1-BAK1^{AAA}/bak1-4* seedlings were treated with 100 nM TAMRA-Pep1 for 10 s (pulse) and imaged at indicated time points (chase). Epidermal cells of root meristematic zone were imaged. Scale bars, 10 µm.

(B) Plasma membrane (PM) vs. intracellular fluorescence intensity measurements of the TAMRA-Pep1 uptake in **(A)**. Individual measurements, average, and SD are indicated as dots, red line, and whiskers, respectively. One-way ANOVA followed by Tukey's test was used to determine significant differences.****P<0.0001.

(C) Representative images of PEPR1-GFP endocytosis visualized by color-based fluorescence intensity coding. Five-day-old *pRPS5A-PEPR1-GFP/pepr1pepr2*, *pRPS5A-PEPR1-GFP/pBAK1-BAK1^{S612A}/bak1-4* and *pRPS5A-PEPR1-GFP/pBAK1-BAK1^{AAA}/bak1-4* seedlings

951 were treated with 100 nM Pep1 for 10 s (pulse) and imaged at indicated time points (chase).
952 Images are a maximum intensity Z-projection. Epidermal cells of root meristematic zone were
953 imaged. Scale bar, 10 µm.
954 **(D)** PM vs. intracellular fluorescence intensity measurements of PEPR1-GFP internalization in
955 **(C)**. Dots, red lines, and whiskers represent individual measurements, red lines, and SD,
956 respectively. One-way ANOVA followed by Tukey's test was used to determine significant
957 differences.****P<0.0001, ***P<0.001, **P<0.01, *P<0.05; n, number of cell analyzed **(B,**
958 **D)**; ns, not significant.

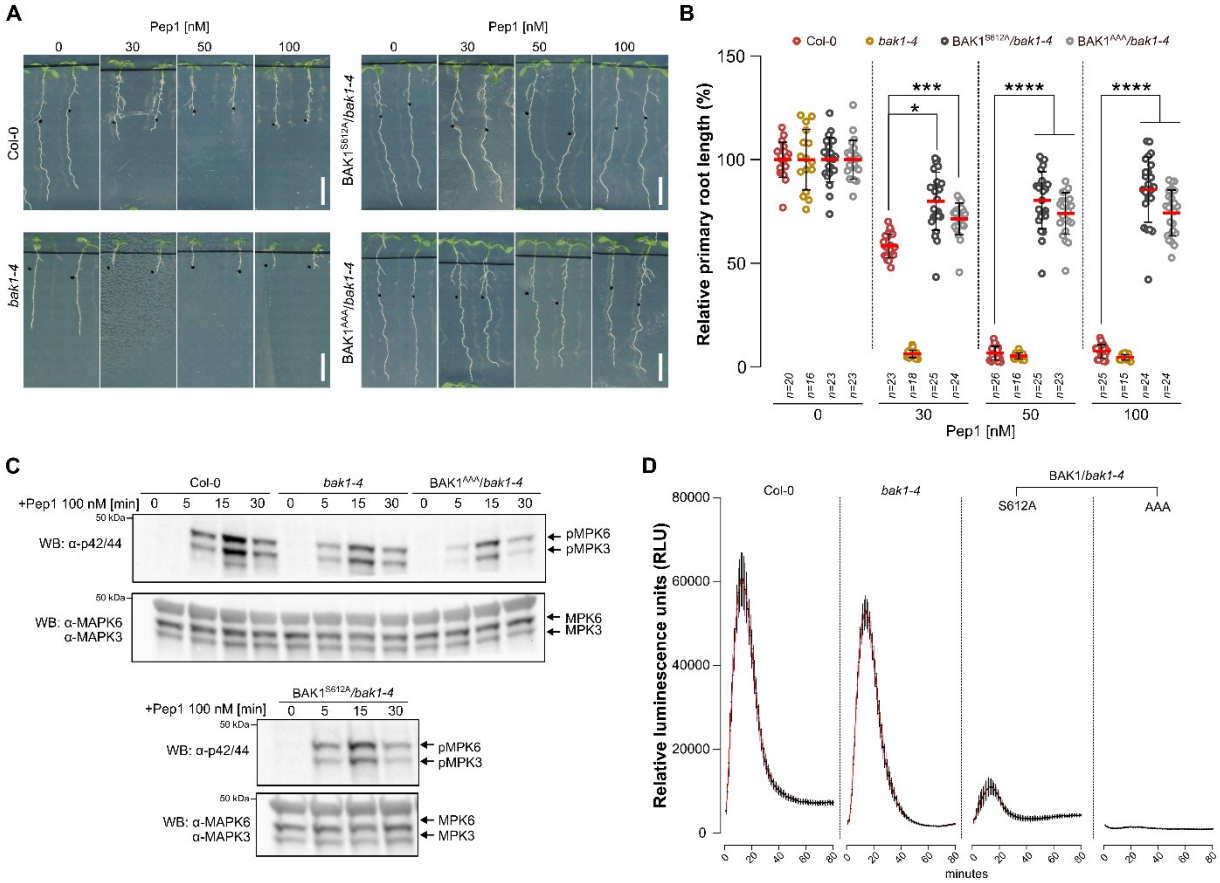

Figure 4. Flagellin-and Pep1-induced signaling pathways require the same BAK1 phosphorylation signature.

(A) Representative images of root growth inhibition caused by different Pep1 concentrations. Seedlings of wild-type Col-0, *bak1-4*, *pBAK1-BAK1^{S612A}/bak1-4* and *pBAK1-BAK1^{AAA}/bak1-4* were grown for 4 days on ½MS agar plates and transferred to ½MS solid media supplemented with different concentrations of Pep1 or water (mock) for a further 3 days. Scale bars, 10 mm.

(B) Primary root length of seedlings in **(A)** presented as relative to the mock-treated control for each genotype. Dots, red lines, and whiskers represent individual measurements, averages, and SD, respectively. The asterisk indicates statistically significant difference analyzed with two-way ANOVA followed by Tukey's test. ****P<0.0001, ***P<0.001, *P<0.05; n, number of seedlings analyzed; ns, not significant.

(C) MAPK activation assay of 5-day-old seedlings in **(A)** treated with 100 nM Pep1 for the indicated time points. Phosphorylated MPK3 (pMPK3) and MPK6 (pMPK6) were detected by Western Blotting (WB) with the α-p42/44 antibody (top). Protein loading is shown by total MPK3 and MPK6 detected with the α-MPK3 and α-MPK6 antibodies (bottom).

(D) Pep1-induced reactive oxygen species (ROS) production. Eight leaf discs from four 5-week-old plants in **(A)** were treated with 100 nM of Pep1. ROS production measured as RLU was detected at the indicated time points. Red lines indicate means ± SD.

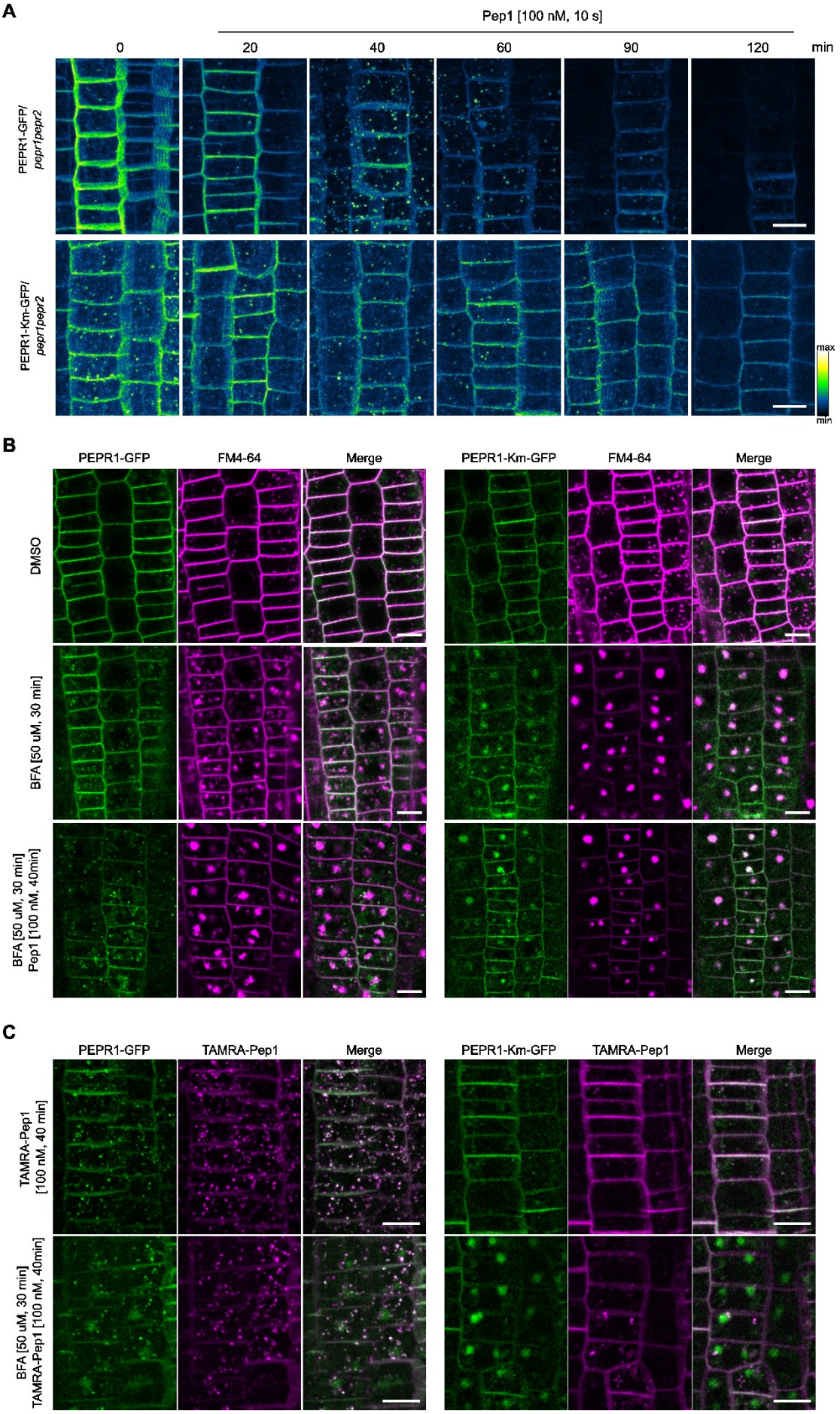
A
Pep1 [100 nM, 10 s]
0
20
40
60
90
120
min
PEPR1-GFP/ pepr1pepr2
PEPR1-Km-GFP/ pepr1pepr2
max
min
B
PEPR1-GFP
FM4-64
Merge
PEPR1-Km-GFP
FM4-64
Merge
DMSO
BFA [50 uM, 30 min]
BFA [50 uM, 30 min] Pep1 [100 nM, 40min]
C
PEPR1-GFP
TAMRA-Pep1
Merge
PEPR1-Km-GFP
TAMRA-Pep1
Merge
TAMRA-Pep1 [100 nM, 40 min]
BFA [50 uM, 30 min] TAMRA-Pep1 [100 nM, 40min]

978

979 **Figure 5. The kinase activity of PEPR1 is required for its endocytosis.**
980 **(A)** Representative images of PEPR-GFP and PEPR1-Km-GFP (PEPR1-kinase mutant- GFP)
981 internalization visualized by color-based fluorescence intensity coding. Five-day-old *pRPS5A-*
982 *PEPR1-GFP/pepr1pepr2* and *pRPS5A-PEPR1-Km-GFP/pepr1pepr2* seedlings were treated
983 with 100 nM of Pep1 for 10 s (pulse) and imaged at the indicated time points (chase). Epidermal
984 cells of root meristematic zone were imaged. Images are maximum intensity Z-projections.
985 Scale bars, 10 µm.
986 **(B, C)** Representative images of PEPR1-GFP/*pepr1pepr2* and PEPR1-Km-GFP/*pepr1pepr2*
987 internalization in the presence of BFA **(B)** and endocytosis of TAMRA-Pep1 in the absence
988 and presence of BFA **(C)**. Seedlings as in **(A)** were treated with DMSO (mock), BFA (50 µM,
989 30 min) and Pep1 (100 nM, 40 min) after pre-treatment with BFA (50 µM, 30 min) **(B)**.
990 Seedlings as in **(A)** were treated with TAMRA-Pep1 (100 nM, 40 min) or TAMRA-Pep1
991 (100 nM, 40 min) after pre-treatment with BFA (50 µM, 30 min) **(C)**. Epidermal cells of the
992 root meristematic zone were imaged. Images are maximum Z-projections. 2 µM FM64 (*N*-(3-
993 triethylammoniumpropyl)-4-(6-(4-(diethylamino) phenyl) hexatrienyl) pyridinium dibromide)
994 dye was used to visualize general endocytosis in **(B)**. Scale bars, 10 µm.
995

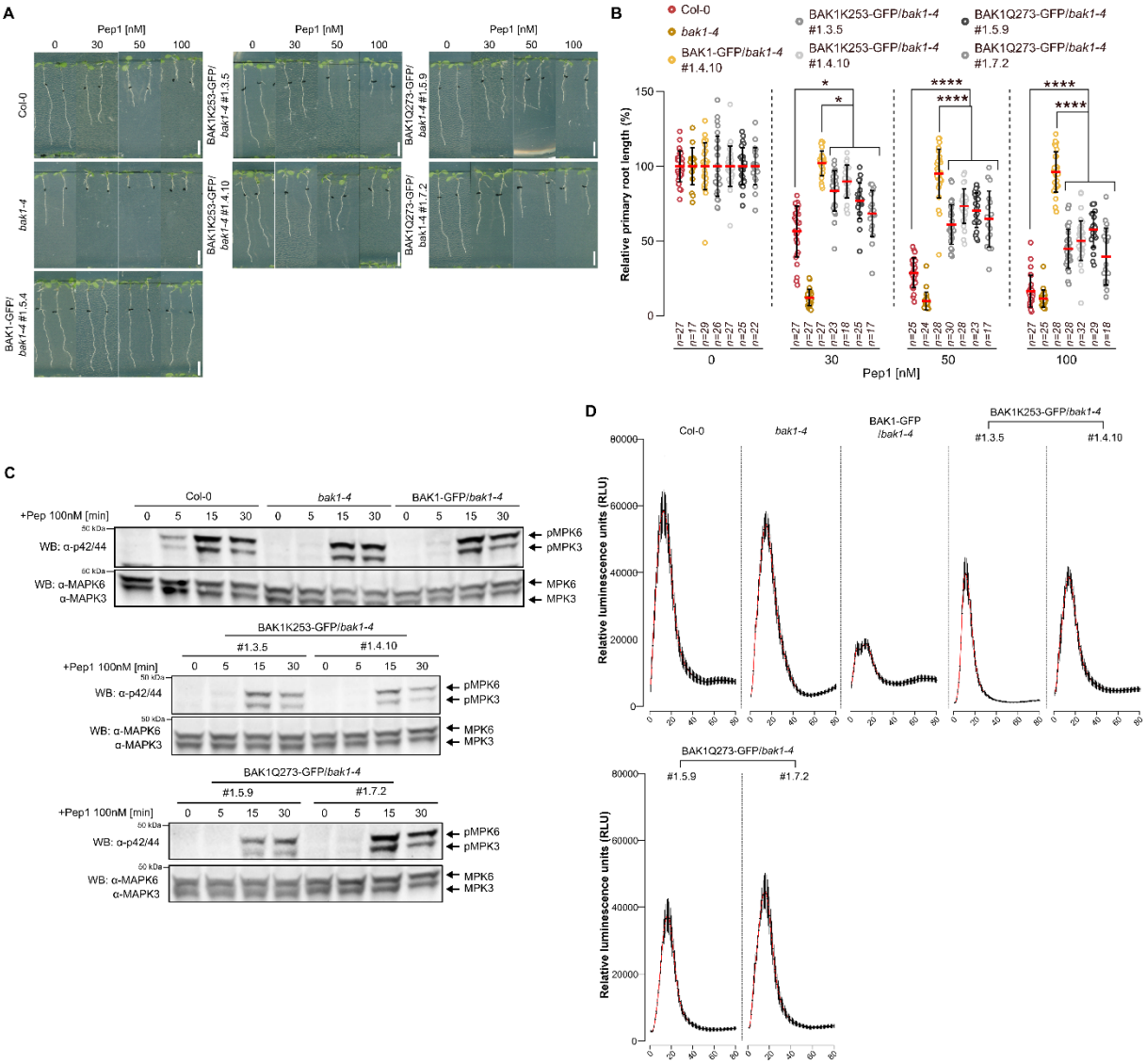

Figure 6. Arabidopsis plants expressing BAK1K253-GFP and BAK1Q273-GFP are partially sensitive to exogenous Pep1.

(A) Representative images of root growth inhibition caused by different Pep1 concentrations. Seedlings of wild-type Col-0, *bak1-4*, *pBAK1-BAK1-GFP/bak1-4*, and two independent transgenic lines of each *pBAK1-BAK1K253-GFP/bak1-4* and *pBAK1-BAK1Q273-GFP/bak1-4* were grown for 4 days on ½MS agar plates and then transferred to a ½MS solid media supplemented with different concentrations of Pep1 or water (mock) for a further 3 days. Scale bars, 10 mm.

(B) Primary root length of seedlings in **(A)** presented as relative to the mock-treated control for each genotype. Dots, red lines, and whiskers represent individual measurements, averages, and SD. Statistically significant difference analyzed with two-way ANOVA followed by Tukey's test; ****P<0.0001, *P<0.05; n, number of seedlings analyzed.

1009 **(C)** MAPK activation assay after Pep1 application of 5-day-old seedlings as in **(A)** treated with
1010 100 nM Pep1 for the indicated time points. Phosphorylated MPK3 (pMPK3) and MPK6
1011 (pMPK6) were detected by Western Blotting (WB) with the α-p42/44 antibody (top). Protein
1012 loading is shown by total MPK3 and MPK6 detected with the α-MPK3 and α-MPK6 antibodies
1013 (bottom).
1014 **(D)** Pep1-induced reactive oxygen species (ROS) production. Eight leaf discs from four 5-
1015 week-old plants in (A) were treated with 100 nM of Pep1. ROS production measured as RLU
1016 was detected at the indicated time points. Red lines indicate mean ± SD.
1017

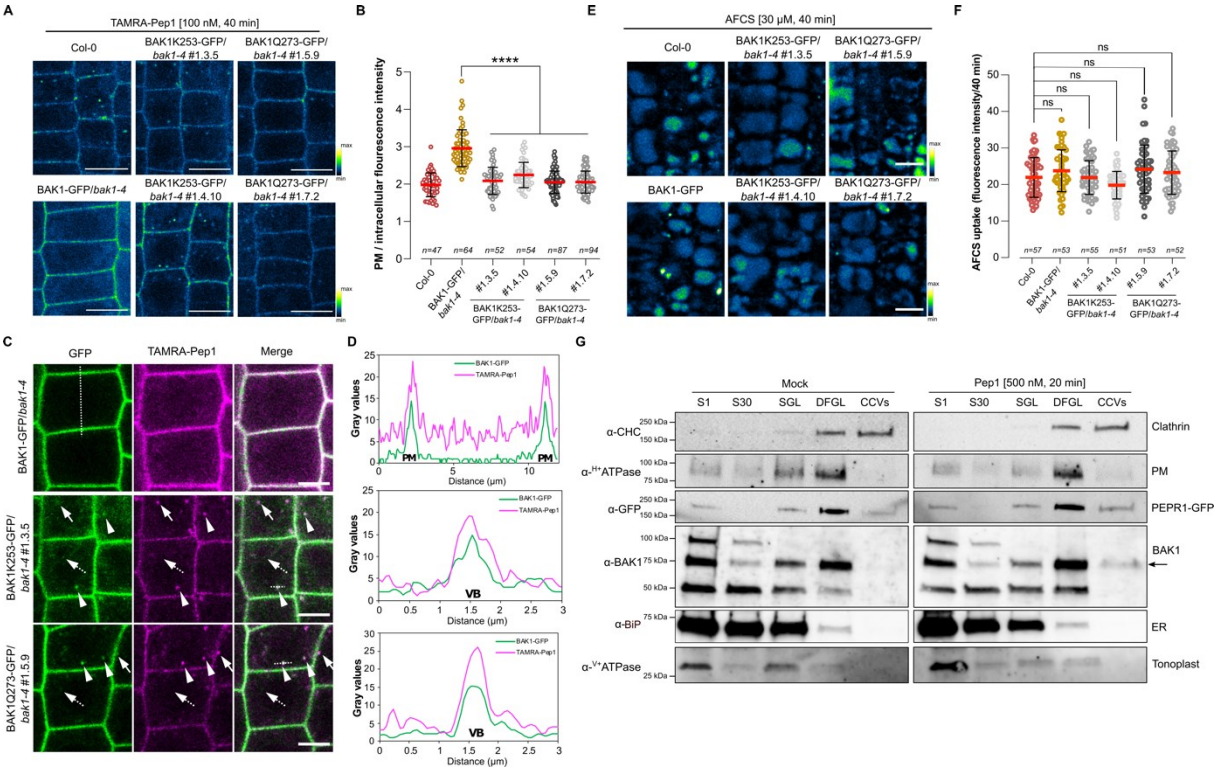

Figure 7. BAK1 and PEPR1 are likely co-internalized.

(A, E) Representative images of TAMRA-Pep1 **(A)** and AFCS **(E)** root uptake visualized by color-based fluorescence intensity coding. Five-day-old seedlings of wild-type Col-0, *bak1-4*, *pBAK1-BAK1-GFP/bak1-4*, *pBAK1-BAK1K253-GFP/bak1-4* and *pBAK1-BAK1Q273-GFP/bak1-4* were treated with 100 nM TAMRA-Pep1 for 10 s (pulse) and with 40 μM of AFCS for 20 min (pulse), respectively, and imaged after 40 min (chase). Epidermal cells of root meristematic zone were imaged. Scale bars, 10 μm.

(B, F) Fluorescence intensity measurements of the plasma membrane (PM) vs. intracellular compartments of the TAMRA-Pep1 uptake in **(A)** and AFCS uptake **(E)** after 40 min chase. Dots, red lines, and whiskers represent individual measurements, averages, and SD. The one-way ANOVA followed by Tukey's test was used to determine significant differences. ****P<0.0001; ns, not significant; n, number of cell analyzed.

(C) Co-localization of BAK1-GFP and TAMRA-Pep1. Five-day-old *pBAK1-BAK1-GFP/bak1-4*, *pBAK1-BAK1K253-GFP/bak1-4* and *pBAK1-BAK1Q273-GFP/bak1-4* seedlings were treated with 100 nM of TAMRA-Pep1 for 10 s (pulse) and imaged after 40 min (chase). Arrowheads, arrows and dashed-arrows indicate co-localizing puncta, TAMRA-Pep1 puncta only and BAK1-GFP puncta only, respectively. Scale bars, 10 μm.

(D) Line plot of the BAK1-GFP and TAMRA-Pep1 fluorescent signals of the dashed line in **(C)** VB, vesicle body; PM, plasma membrane. Epidermal cells of root meristematic zone were imaged.

1039 **(G)** Co-localization between PEPR1 and BAK1 in clathrin-coated vesicles (CCVs). CCVs were
1040 prepared from total plant extracts of 10-day-old *pRPS5A-PEPR1-GFP*/*pepr1pepr2* seedlings.
1041 Samples were collected during CCV purification and subjected to Western Blotting (WB) with
1042 antibodies against clathrin heavy chain (CHC), GFP, BAK1, and various subcellular organelle
1043 marker proteins. S1, supernatant after centrifugation at 1000*g*; S30, supernatant after
1044 centrifugation at 30,000*g*; SGL, sucrose step gradient load; DFGL, deuterium oxide/ficoll
1045 gradient load; CCVs, CCV-containing fraction. The following antibodies were used as
1046 organelle- or compartment-specific markers: α-H-ATPase (PM), α-V-ATPase (vacuole), and
1047 α-BiP (ER; endoplasmic reticulum).
1048

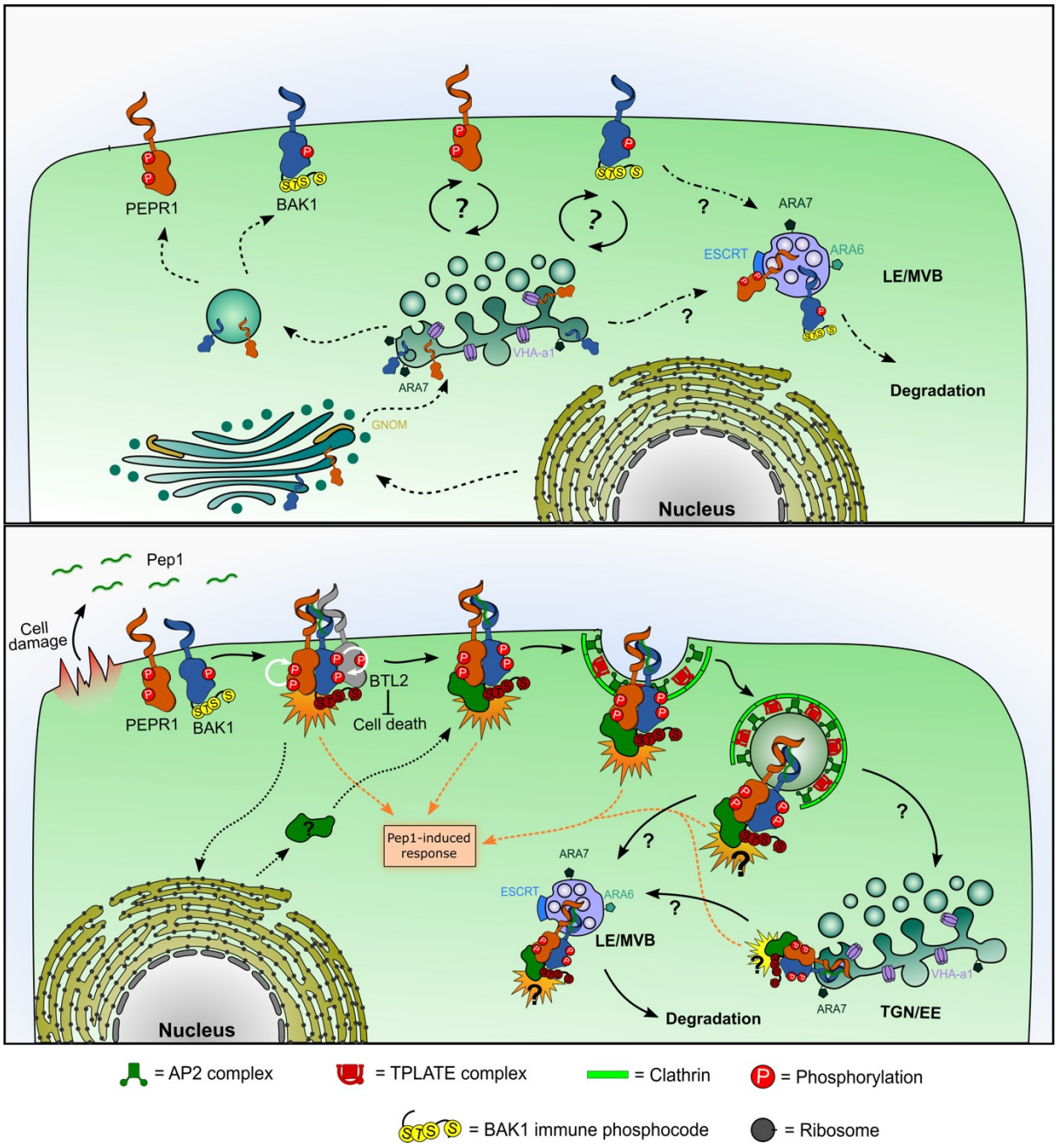

Figure 8. Proposed model of BAK1-PEPR1 activation and endocytosis.

(A) In the non-elicited state, BAK1 and PEPR1 are delivered to the plasma membrane (PM) via the secretory pathway (dashed lines), passing through the endoplasmic reticulum (ER), Golgi apparatus, and trans-Golgi network/early endosomes (TGN/EE). Once at the PM, BAK1 and PEPR1 may undergo recycling. However, neither receptor is abundant in brefeldin A (BFA) bodies, suggesting that, if recycling occurs, it proceeds through a BFA-insensitive route. Ultimately, BAK1 and PEPR1 can be degraded (dash-dot lines) either by direct trafficking from the PM to late endosomes/multivesicular bodies (LE/MVBs) or via the TGN/EE and then to LE/MVBs for delivery to the vacuole, where they are degraded.

1060 (B) Upon Pep1 perception, PEPR1 dimerizes with BAK1 and trans-phosphorylates it. This
1061 presumably triggers phosphorylation of BAK1 at residues S602, T603, S604, and S612, which
1062 are required for Pep1-induced immune responses and for PEPR1 endocytosis. In parallel, BAK1
1063 promotes increased PEPR1 phosphorylation, whereas PEPR1 subsequently attenuates BAK1
1064 activity. Concurrently, BAK1 phosphorylates BAK-TO-LIFE 2 (BTL2), thereby suppressing
1065 BTL2-mediated autoimmunity. Pep1 signaling also induces the transcription and translation of
1066 an unknown factor that may be required for endocytosis of the PEPR1–Pep1–BAK1 complex.
1067 PEPR1 is internalized together with BAK1 via clathrin-mediated endocytosis. After
1068 internalization, the complex is targeted directly to LE/MVBs or traffics via the TGN/EE and
1069 then to LE/MVBs for delivery to the vacuole for degradation.

Supplemental information

Endocytosis of the damage-associated molecular pattern receptor PEPR1 is BAK1-dependent

Lucas Alves Neubus Claus[1,2,*], Fausto Andrés Ortiz-Morea[1,2,3,4], Shao-Li Yang[1,2], Shweta Yekondi[1,2], Xiangyu Xu[1,2], In-Cheol Yeo[3], Isabelle Vanhoutte[1,2], Nemanja Vukašinović[1,2], Qian Ma[1,2], Ive De Smet[1,2], Ping He[3], Libo Shan[3], and Eugenia Russinova[1,2,*]

[1]Department of Plant Biotechnology and Bioinformatics, Ghent University, 9052 Ghent, Belgium
[2]Center for Plant Systems Biology, VIB, 9052 Ghent, Belgium
[3]Department of Molecular, Cellular, and Developmental Biology, University of Michigan, Ann Arbor, Michigan 48109, USA
[4]Agricultural Engineering Program, University of the Amazon, Florencia 180002622, Colombia

***Correspondence: Lucas Alves Neubus Claus (lucas.claus13@gmail.com) and Eugenia Russinova (eurus@psb.vib-ugent.be)**

The supplemental file includes 9 supplemental figures and 1 supplemental table

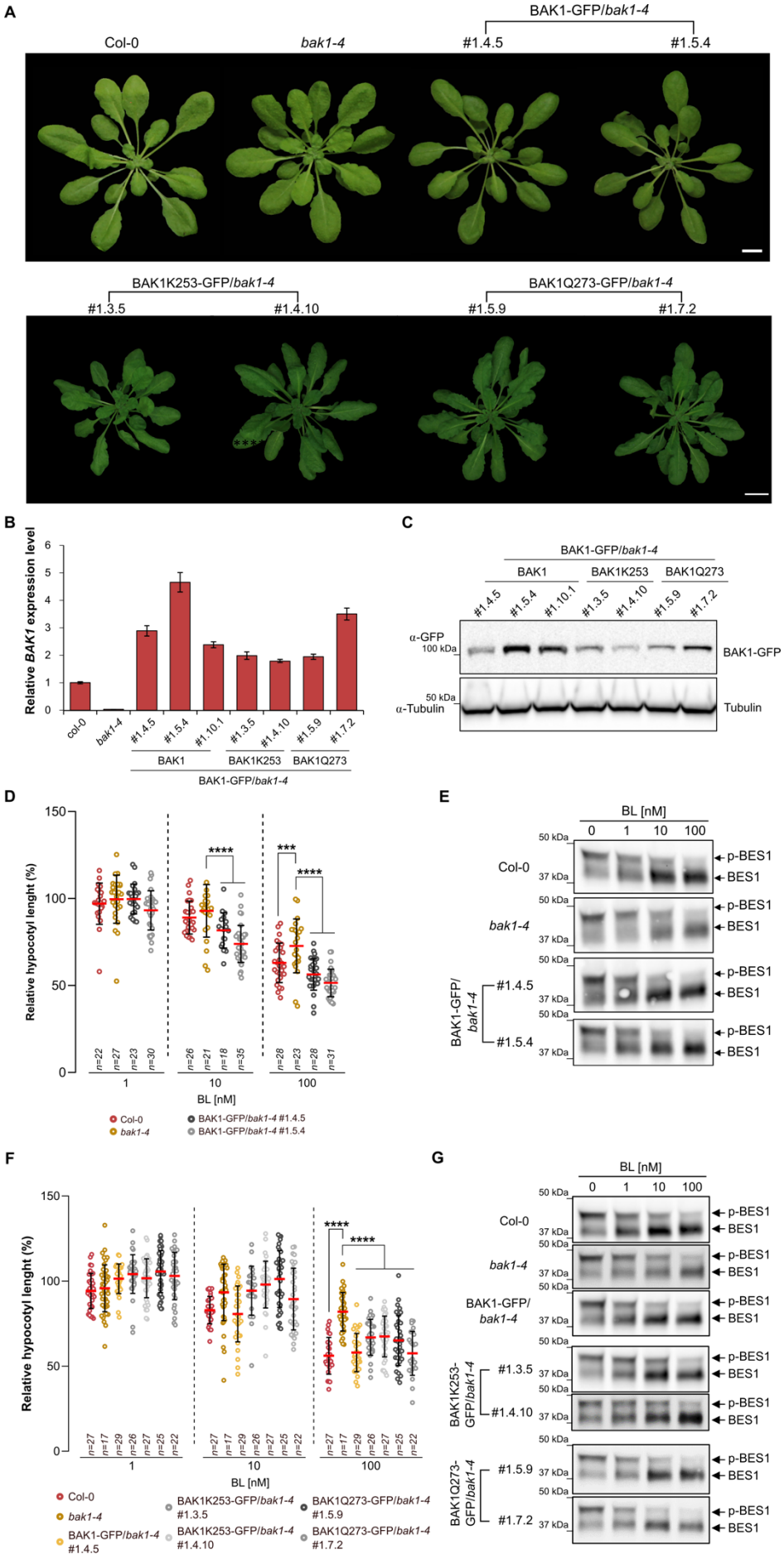
A
BAK1-GFP/bak1-4
Col-0
bak1-4
#1.4.5
#1.5.4
BAK1K253-GFP/bak1-4
#1.3.5
#1.4.10
BAK1Q273-GFP/bak1-4
#1.5.9
#1.7.2
B
Relative BAK1 expression level
col-0
bak1-4
BAK1
BAK1K253
BAK1Q273
BAK1-GFP/bak1-4
C
α-GFP
100 kDa
BAK1-GFP
50 kDa
α-Tubulin
Tubulin
D
Relative hypocotyl lenght (%)
BL [nM]
Col-0
bak1-4
BAK1-GFP/bak1-4 #1.4.5
BAK1-GFP/bak1-4 #1.5.4
E
BL [nM]
Col-0
bak1-4
BAK1-GFP/bak1-4
p-BES1
BES1
F
Relative hypocotyl lenght (%)
BL [nM]
BAK1K253-GFP/bak1-4 #1.3.5
BAK1K253-GFP/bak1-4 #1.4.10
BAK1Q273-GFP/bak1-4 #1.5.9
BAK1Q273-GFP/bak1-4 #1.7.2
G
BAK1K253-GFP/bak1-4
BAK1Q273-GFP/bak1-4

Supplemental Figure 1. The C-terminal BAK1-GFP tag did not impair BR responses.

(A) Representative images of 4-week-old plants of the indicated genotypes. Scale bars, 1 cm.

(B) Real-time quantitative reverse transcription PCR (qRT-PCR) analysis of *BAK1*. Total RNA was isolated from 7-day-old seedlings of two or three independent transgenic lines. Transcript levels were normalized to *GAPDH* and *ACTIN2* gene expression and three biological with three technical replicates each were quantified. Data are means ± SD.

(C) Total proteins isolated from 7-day-old seedlings and detected by Western Blotting (WB) with α-GFP antibodies to detect the BAK1-GFP. Numbers indicate individual transgenic lines. α-tubulin antibodies were used to equilibrate protein loading.

(D, F) Hypocotyl length measurements after brassinolide (BL) treatment relative to the mock (DMSO). Seedlings of wild-type Col-0, *bak1-4* and two independent transgenic lines of each *pBAK1-BAK1-GFP*/*bak1-4*, *pBAK1-BAK1K253-GFP*/*bak1-4,* and *pBAK1-BAK1Q273-GFP*/*bak1-4* were grown for 4 days in the dark on ½MS agar plates supplemented with increasing concentrations of BL. Dots, red lines, and whiskers represent individual measurements, averages, and SD, respectively. Statistically significant difference were analyzed with two-way ANOVA followed by a Tukey's test. ***$P<0.001$; ****$P<0.0001$; n, number of seedlings analyzed.

(E, G) BES1 dephosphorylation assay after BL treatment. Five-day-old seedlings of wild-type Col-0, *bak1-4* and of two independent transgenic lines of each *pBAK1-BAK1-GFP*/*bak1-4*, *pBAK1-BAK1K253-GFP*/*bak1-4,* and *pBAK1-BAK1Q273-GFP*/*bak1-4* were treated with increasing concentrations of BL for 1 h. BES1 was detected by WB with the α-BES1 antibody and discrimination between phosphorylated (p-BES1) and unphosphorylated BES1 was based on the protein size shift.

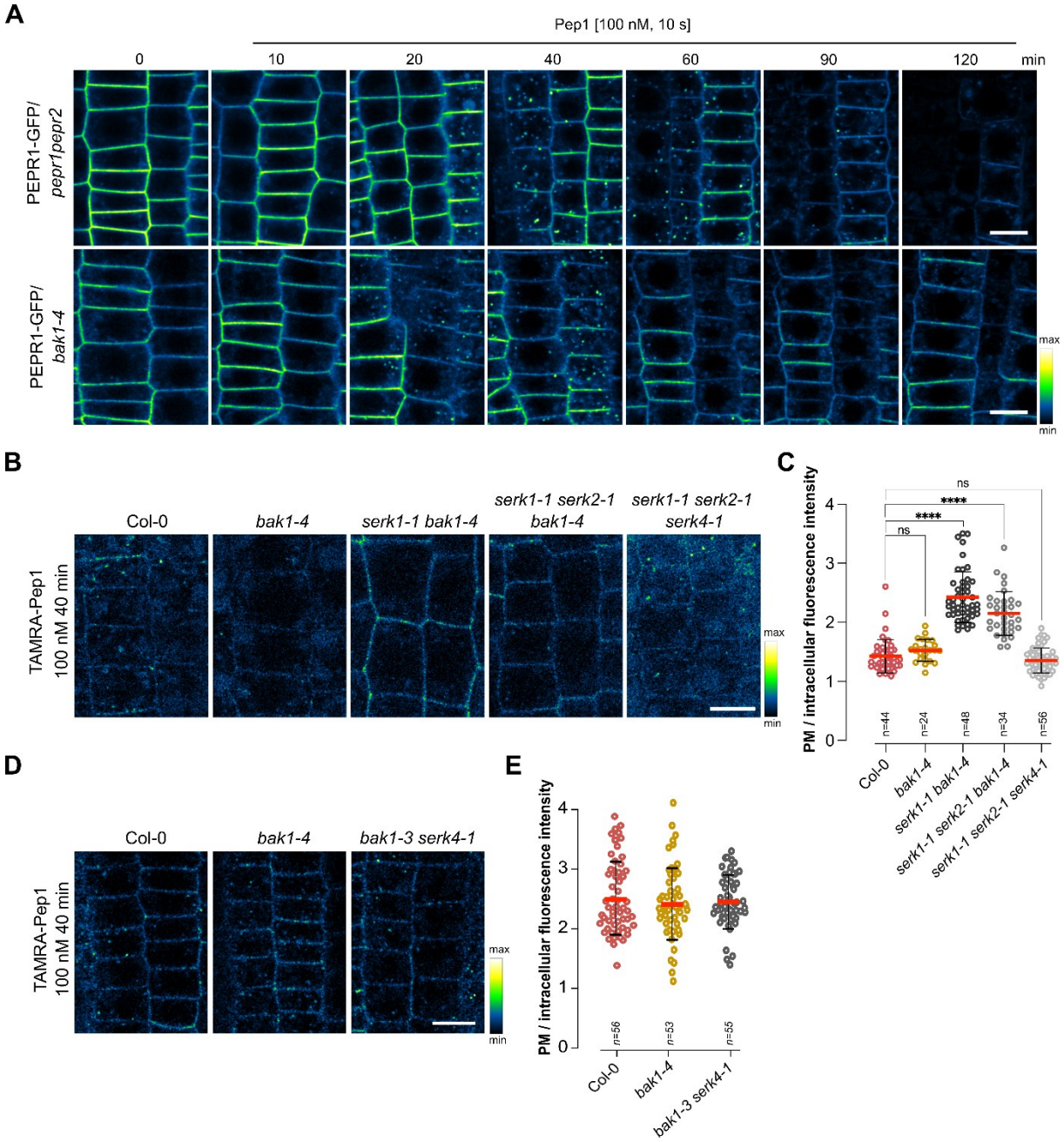

Supplemental Figure 2. PEPR1 endocytosis requires SERKs.

(A) Representative images of PEPR1-GFP endocytosis in roots of *pepr1pepr2* and *bak1-4* mutants. Five-day-old *pRPS5A-PEPR1-GFP/pepr1pepr2* and *pRPS5A-PEPR1-GFP/bak1-4* seedlings were treated with 100 nM Pep1 for 10 s (pulse) and imaged at the indicated time points (chase).

(**B, D**) TAMRA-Pep1 root uptake visualized by color-based fluorescence intensity coding. 5-day-old wild-type Col-0*, bak1-4, serk1-1bak1-4*, *serk1-1serk2-1bak1-4* and *serk1-1serk2-1serk4-1* (**B**) and Col-0, *bak1-4* and *bak1-3serk4-1* (**D**) seedlings were treated with 100 nM of TAMRA-Pep1 for 10 s (pulse) and imaged after 40 min (chase). Homozygous seedlings for the triple mutants were selected based on phenotype.

(C, E) Plasma membrane (PM) vs. intracellular fluorescence intensity measurements of the TAMRA-Pep1 uptake in **(B, D)**. Dots, red lines, and whiskers represent individual measurements, averages, and SD, respectively. Statistically significant differences were analyzed with one-way ANOVA followed by Tukey's test. ****$P<0.0001$; ns, not significant; *n*, number of cell analyzed. Epidermal cells of root meristematic zone were imaged (**A, B, D**). Scale bars, 10 µm (**A, B, D**).

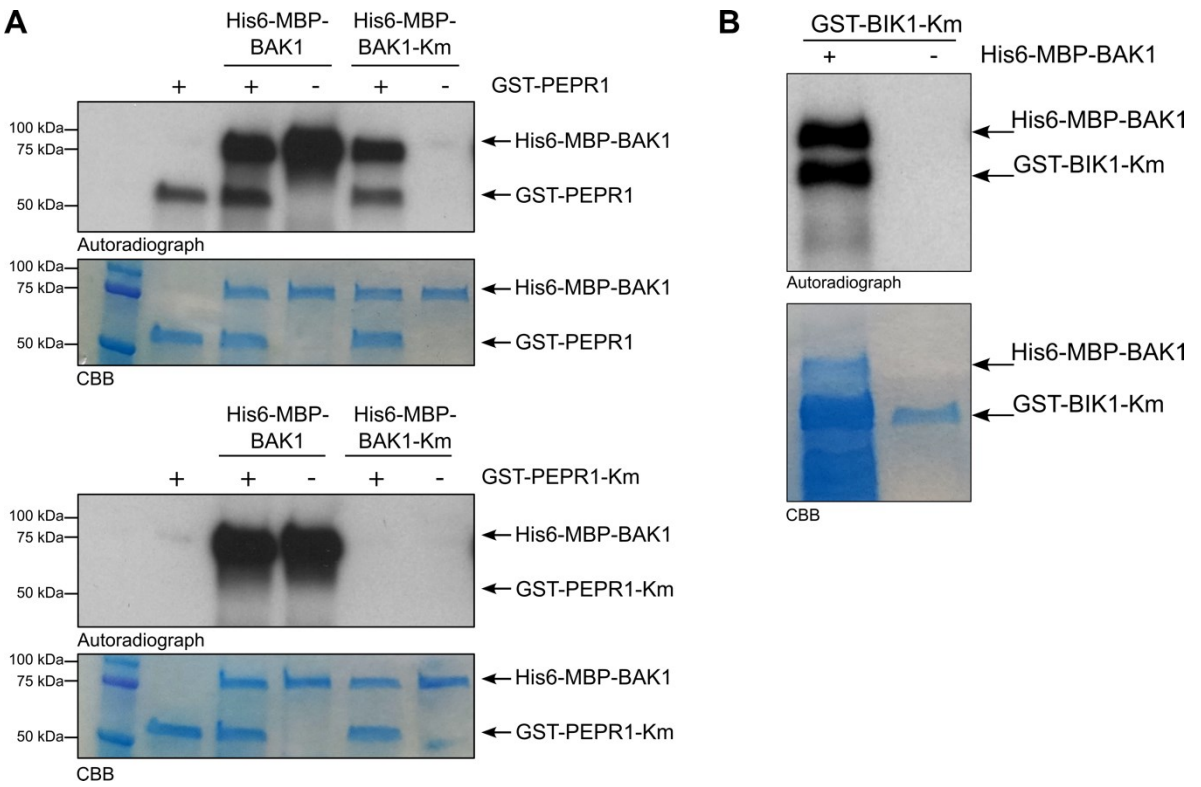

Supplemental Figure 3. BAK1 cannot trans-phosphorylate PEPR1 *in vitro.*

(**A**) The cytoplasmic domains of BAK1 and PEPR1, and their respective kinase-dead mutant (Km) versions of PEPR1-Km (K855E) and BAK1-Km (D416N) tagged with either glutathione S-transferase (GST) or His6-maltose-binding protein (MBP) were produced in bacteria. *In vitro* kinase assay performed with a single or combined recombinant proteins as indicated. CBB, Coomassie Brilliant Blue.

(**B**) His6-MBP-BAK1 can phosphorylate the inactive BIK1 kinase (BIK1-Km). For the *in vitro* kinase assay a single or recombinant proteins together were used, as indicated. Protein loading was controlled by Coomassie Brilliant Blue (CBB).

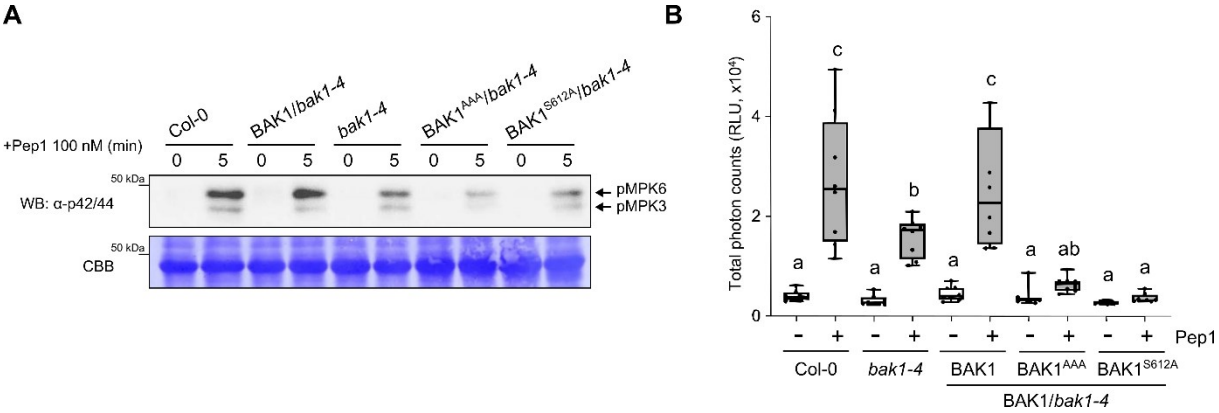

Supplemental Figure 4. MAPK activation and ROS burst after Pep1 treatment were impaired in the BAK1^{S612A} and BAK1^{AAA} mutants

(**A**) Pep1-mediated MAPK activation was compromised in BAK1^{S612A} and BAK1^{AAA} mutants as shown in *bak1-4* mutant. 9-day-old seedlings of wild-type (Col-0), *pBAK1-BAK1*/*bak1-4*, *pBAK1-BAK1^{S612A}*/*bak1-4*, and *pBAK1-BAK1^{AAA}*/*bak1-4* were treated with 100 nM Pep1 and with mock (water) for 5 min. MAPK activation was analyzed with α-pERK1/2 antibodies (top), and protein loading is shown by CBB staining for RBC (bottom).

(**B**) The BAK1^{S612A} and BAK1^{AAA} mutants showed compromised Pep1-induced ROS burst. Leaf discs (n = 8) from 4-week-old soil-grown plants were treated with or without 300 nM Pep1, and ROS production was measured as relative light units (RLUs) by a luminometer. Data represent mean ± SEM

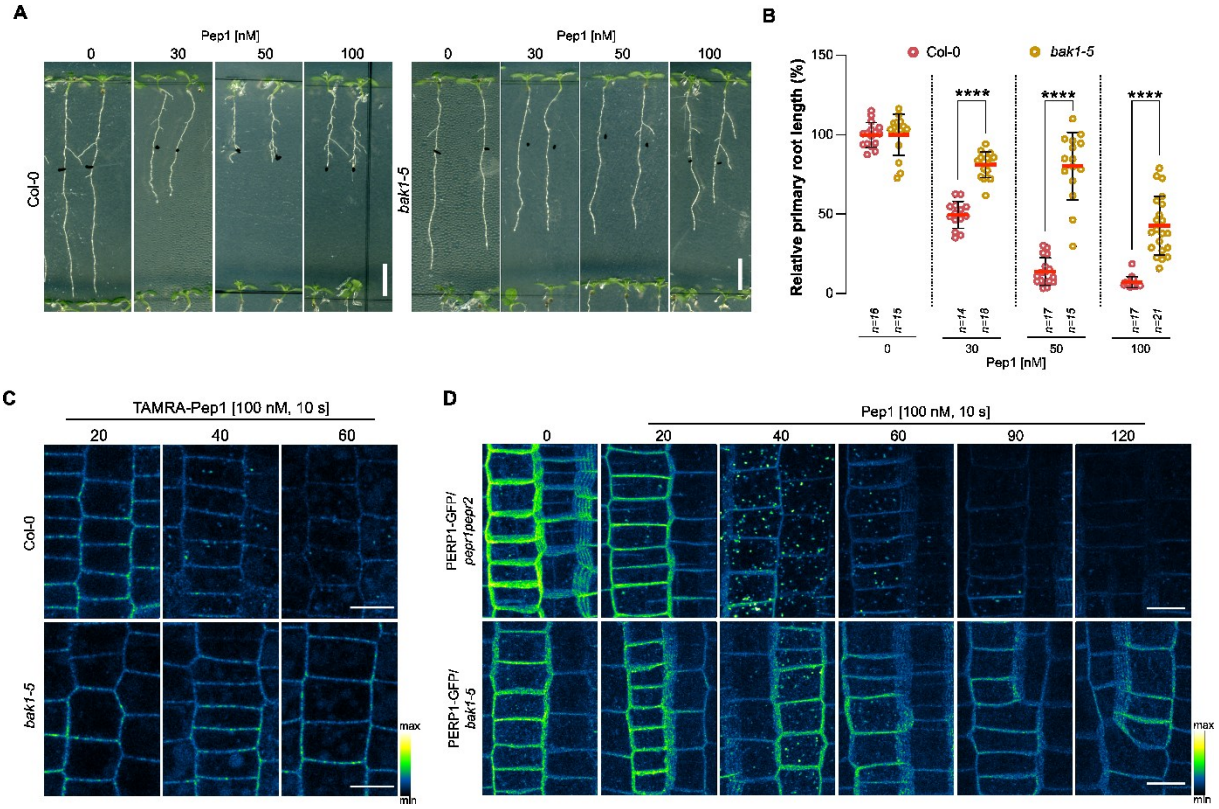

Supplemental Figure 5. The hypoactive kinase BAK1-5 disrupts PEPR1 endocytosis and signaling.

(A) Representative images of the root growth inhibition caused by different Pep1 concentrations. Seedlings of wild-type Col-0 and *bak1-5* were grown for 4 days on ½MS agar plates and transferred to ½MS agar media supplemented with different concentrations of Pep1 or water (mock) for 3 days. Scale bars, 10 mm.

(B) Primary root length of seedlings in **(A)** presented as relative to the mock-treated control for each genotype. Dots, red lines, and whiskers represent individual measurements, averages, and SD, respectively. The two-way ANOVA followed by Tukey's test was used to determine significant differences. ****P<0.0001; n, number of seedlings analyzed.

(C, D) Representative images of TAMRA-Pep1 root uptake **(C)** and PEPR1-GFP endocytosis **(D)** in the *bak1-5* mutant visualized by color-based fluorescence intensity coding. Five-day-old seedlings of wild-type Col-0 and *bak1-5* **(C)**, and *pRPS5A-PEPR1-GFP*/*pepr1pepr2* and *pRPS5A-PEPR1-GFP*/*bak1-5* were treated with 100 nM of TAMRA-Pep1 **(C)** and 100 nM Pep1 **(D)** for 10 s and imaged at indicated time points (chase). Epidermal cells of root meristematic zone were imaged. Images are maximum intensity Z-projections. Scale bars, 10 µm.

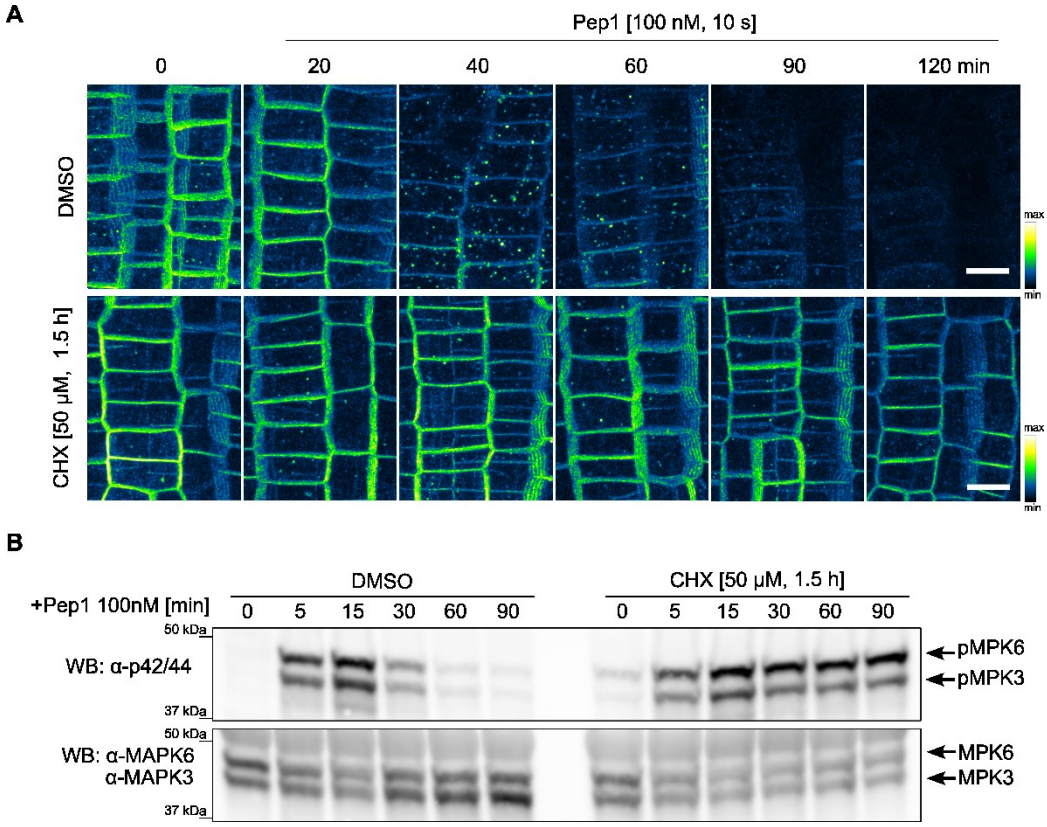

Supplemental Figure 6. Cycloheximide (CHX) blocks PEPR1-GFP endocytosis and affects Pep1-triggered MAPK activation

(A) Representative images of PEPR1-GFP internalization visualized by color-based fluorescence intensity coding in the presence of CHX. Five-day-old *pRPS5A-PEPR1-GFP/pepr1pepr2* seedlings were pre-treated with DMSO (mock) and CHX (50 µM, 1.5 h) followed by application of 100 nM Pep1 for 10 s (pulse) and imaged at the indicated time points (chase). Epidermal cells of root meristematic zone were imaged. Images are maximum intensity Z-projections. Scale bars, 10 µm.

(B) MAPK activation assay after Pep1 treatment in the presence of CHX. Five-day-old wild-type Col-0 seedlings were pre-treated with DMSO (mock) or CHX (50 µM, 1.5 h) followed by application of 100 nM Pep1 for the indicated time points. Phosphorylated MPK3 (pMPK3) and MPK6 (pMPK6) were detected by Western Blotting (WB) with α-p42/44 antibody (top). Protein loading of total MPK3 and MPK6 was detected with the α-MPK3 and α-MPK6 antibodies (bottom).

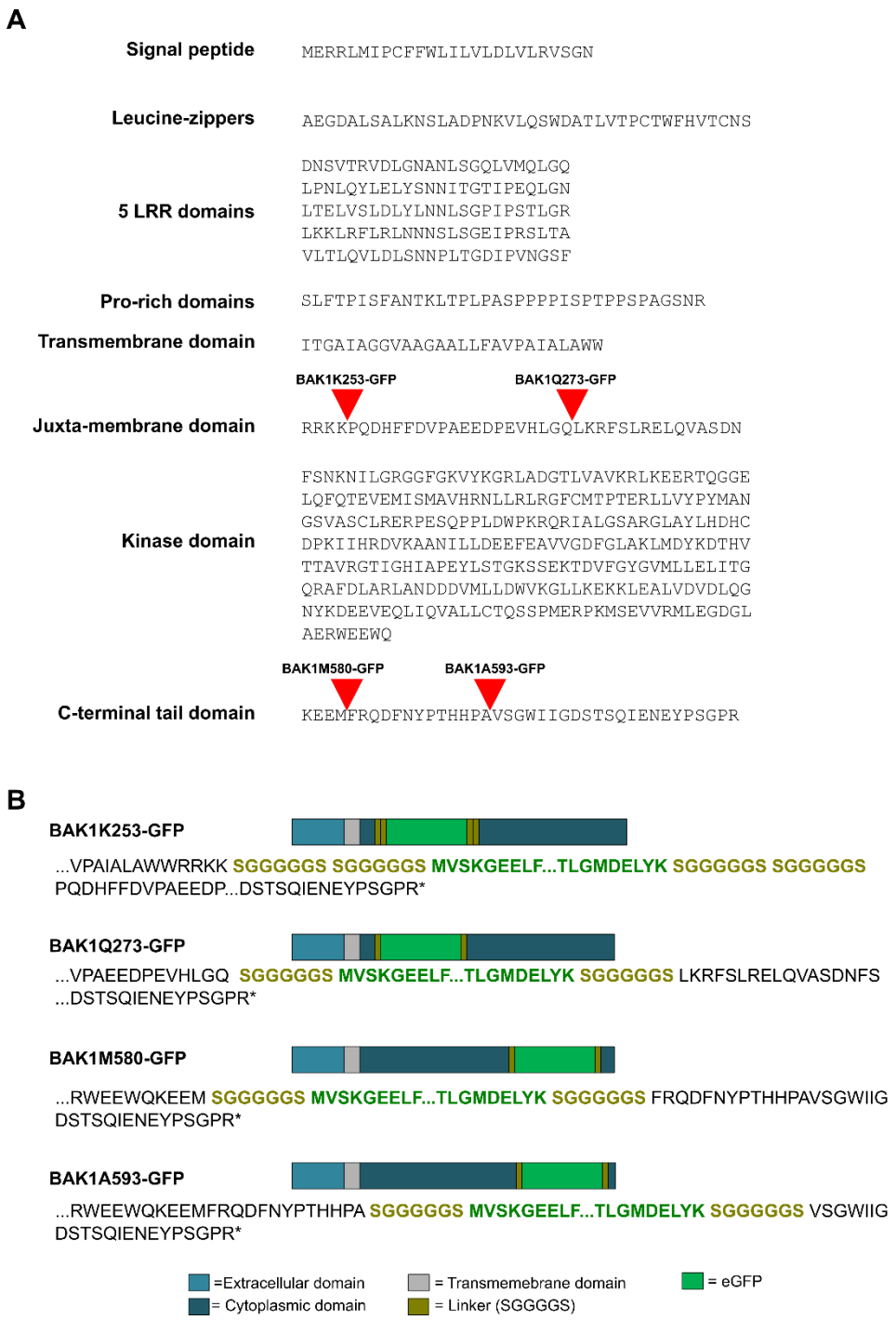

Supplemental Figure 7. Schematic representation of the different constructs containing GFP-tagged BAK1.

(A) Amino acid sequences of the different BAK1 protein domains. The positions of the GFP tags are indicated with red triangle. LRR, leucine-rich repeat.

(B) Schematic representation of the tagged BAK1-GFP lines with the detailed amino acid sequences of the insertional junction regions.

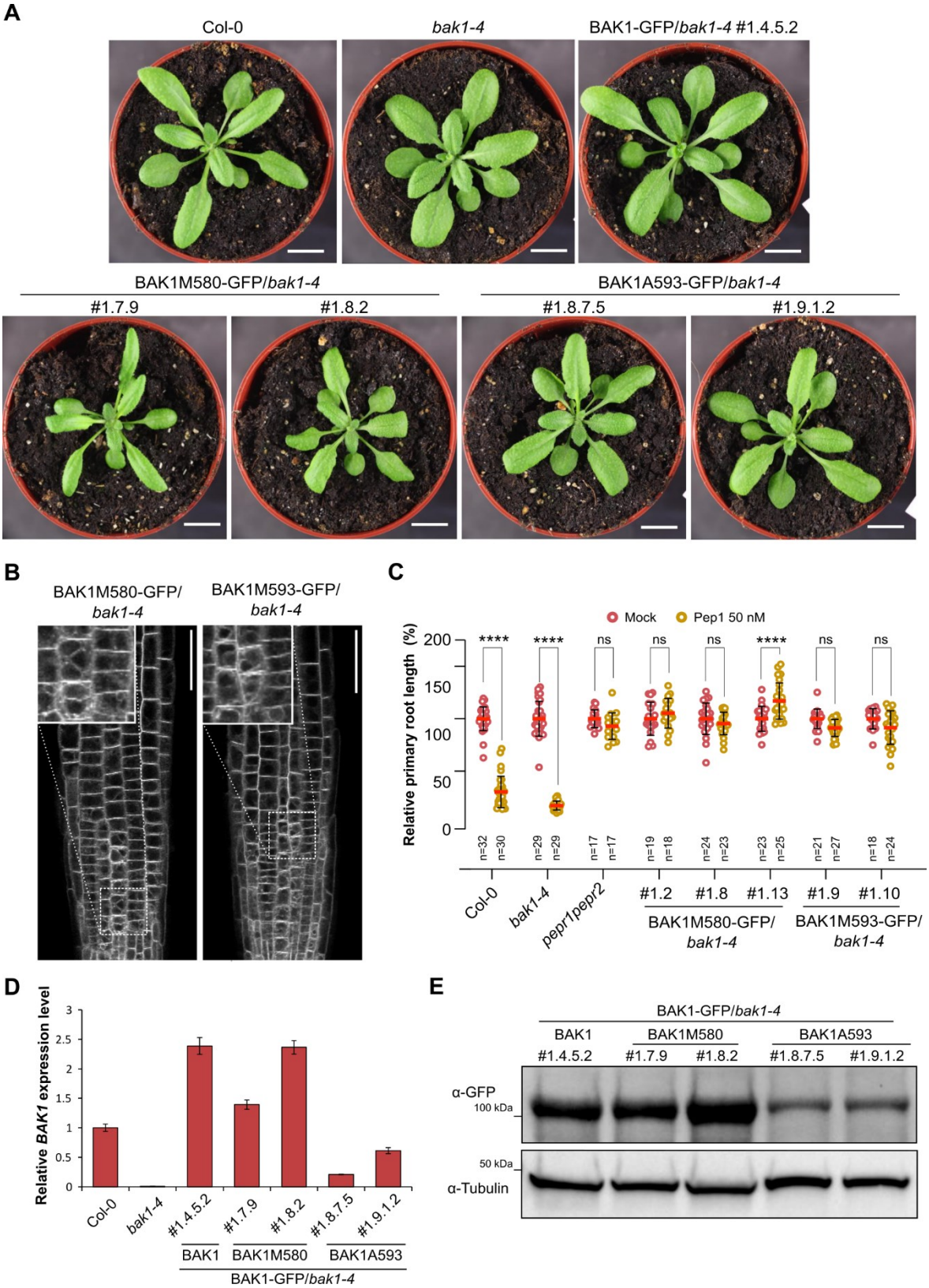

Supplemental Figure 8. GFP insertional mutagenesis screen for functional BAK1-GFP-expressing Arabidopsis lines.

(A) Representative images of 4-week-old T3 plants of the indicated genotypes. Scale bars, 1 cm.

(B) Subcellular localization of BAK1-GFP in different GFP insertion lines. Root meristems of 5-day-old seedlings were imaged. Scale bars, 10 µm.

(C) Relative primary root length of seedlings of the indicated genotypes grown for 4 days on ½MS agar plates and transferred to ½MS solid media supplemented with 50 nM Pep1 or water (mock) for 3 days. Dots, red lines, and whiskers represent individual measurements, averages, and SD, respectively. The two-way ANOVA followed by Tukey's test was used to determine significant differences.****$P<0.0001$; ns, not significant; *n*, number of seedlings analyzed.

(**D**) Real-time quantitative reverse transcription PCR (qRT-PCR) analysis of *BAK1*. Total RNA was isolated from 7-day-old seedlings of two independent transgenic lines. Transcript levels were normalized to *UBQ* gene with three technical replicates of each were quantified. Data are means ± SD

(**E**) Total proteins isolated from 7-day-old seedlings and detected by Western Blotting (WB) with α-GFP antibodies to detect the BAK1-GFP. Numbers indicate individual transgenic lines. α-tubulin antibodies were used to equilibrate protein loading.

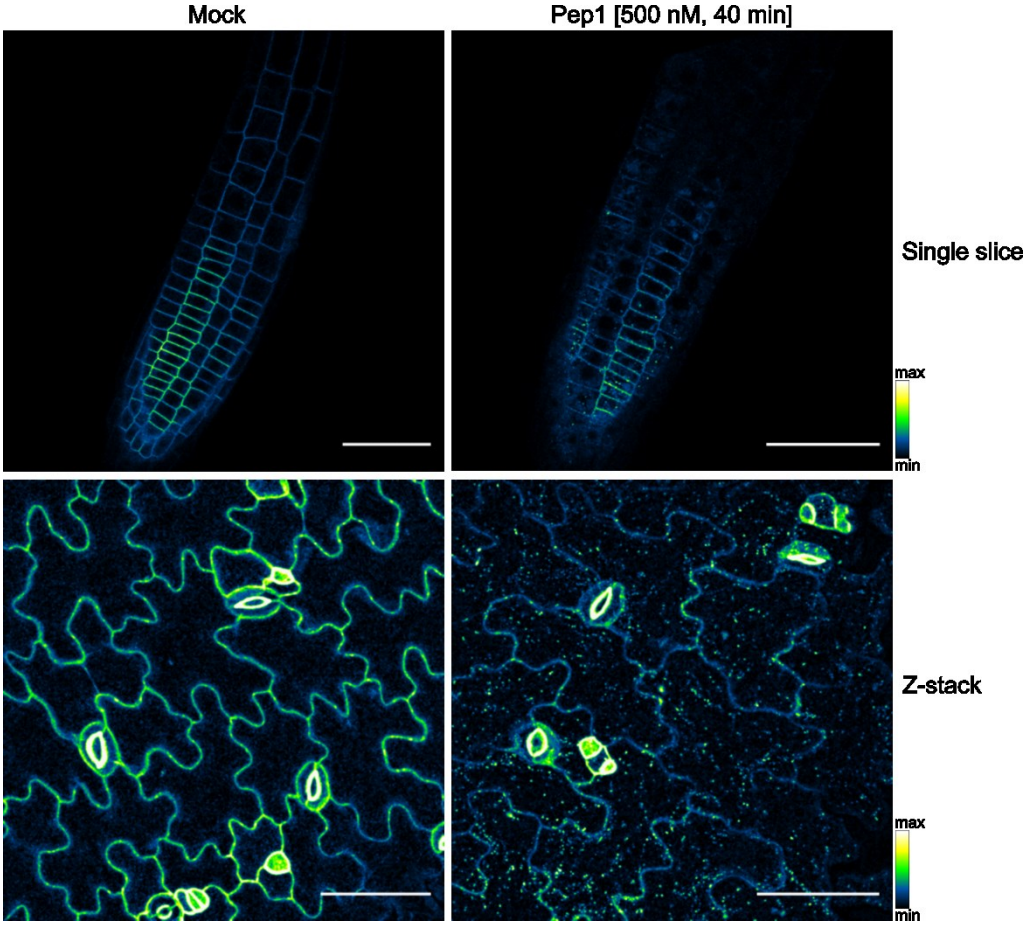

Supplemental Figure 9. PEPR1-GFP endocytosis in Arabidopsis root and shoot.
Representative images of PEPR1-GFP internalization visualized by color-based fluorescence intensity coding. Ten-day-old *pRPS5A-PEPR1-GFP*/*pepr1pepr2* seedlings were treated with water (mock) or 500 nM Pep1 for 40 min and root (top) and cotyledon (bottom) were imaged under confocal microscope. Images are maximum intensity Z-projections. Scale bars, 50 µm.

Supplemental Table 1. Primers used in this study

Name	Sequence (5'-3')	Application
UBQ10_Fw	GGCCTTGTATAATCCCTGATGAATAAG	qPCR
UBQ10_Rv	AAAGAGATAACAGGAACGGAAACATAGT	qPCR
GAPDH_Fw	TTGGTGACAACAGGTCAAGCA	qPCR
GAPDH_Rv	AAACTTGTCGCTCAATGCAATC	qPCR
mCtrine_Fw1	ATCATGGCCGACAAGCAGAA	qPCR
mCtrine_Rv1	TCTCGTTGGGGTCTTTGCTC	qPCR
BAK1_qPCR-Fw	GACAACCGCAGTGCGTGGGA	qPCR
BAK1_qPCR-Rv	TCGCGAGGCGAGCAAGATCA	qPCR
serk1-1-LP	ATACACAAAAGTGAAACGGCG	Genotyping
serk1-1-RP	TTAGACGAAGAATTCGAAGCG	Genotyping
serk2-1-LP	GGAAAACTCAGGTGATCCATTAAG	Genotyping
serk2-1-RP	TTAACAGGTGATGCACTGCAC	Genotyping
bak1-4-LP	CAGGGGCTATATGACCAATTG	Genotyping
bak1-4-RP	TCCTATCTCTCCTACACCGCC	Genotyping
serk4-1-LP	TGGCTCAGAAGAAAACCACAG	Genotyping
serk4-1-RP	CTGCTCCACTTCTGTTTCCAC	Genotyping
LBb1_3	ATTTTGCCGATTTCGGAAC	Genotyping
BAK1-Rv-K253	cctcgcccttgctcaccatAGATCCGCCGCCTCCAGAAGATCC GCCGCCTCCAGActtttttccttcgccaccaagct	Cloning
GFP-Fw-K253	agcttggtggcgaaggaaaaagTCTGGAGGCGGCGGATCTTCT GGAGGCGGCGGATCTatggtgagcaagggcgagg	Cloning
GFP-Rv-K253	acatcaaagaagtggtcctgcggTGAGCCTCCTCCGCCTGATGA GCCTCCTCCGCCTGActtgtacagctcgtccatgccg	Cloning
BAK1-Fw2-K253	cggcatggacgagctgtacaagTCAGGCGGAGGAGGCTCATCA GGCGGAGGAGGCTCAccgcaggaccacttctttgatgt	Cloning
BAK1-Attb2-Rv2-K253	TACCCAGCTTTCTTGTACAAAGTGGTCCCCttatcttggac ccgaggggtattc	Cloning
BAK1_Rv-K273	tcctcgcccttgctcaccatAGATCCGCCGCCTCCAGAttgtcctaaat gaacttctgggtcctc	Cloning
GFP_Fw-K273	gaggacccagaagttcatttaggacaaTCTGGAGGCGGCGGATCTa tggtgagcaagggcgagga	Cloning
GFP_Rv-K273	tagttcacgcaatgaaaacctcttcagTGAGCCTCCTCCGCCTGActt gtacagctcgtccatgccg	Cloning
BAK1_Fw2-K273	cggcatggacgagctgtacaagTCAGGCGGAGGAGGCTCActgaa gaggttttcattgcgtgaacta	Cloning

BAK1-Rv-M580	tcctcgcccttgctcaccatAGATCCGCCGCCTCCAGAcatttcctcct tttgccactcttcc	Cloning
GFP-Fw-M580	ggaagagtggcaaaaggaggaaatgTCTGGAGGCGGCGGATCTat ggtgagcaagggcgagga	Cloning
GFP-Rv-M580	ggttgggtagttgaaatcttgtctgaaTGAGCCTCCTCCGCCTGActt gtacagctcgtccatgccg	Cloning
BAK1-Fw2-M580	cggcatggacgagctgtacaagTCAGGCGGAGGAGGCTCAttcag acaagatttcaactacccaacc	Cloning
BAK1_Rv-A593	tcctcgcccttgctcaccatAGATCCGCCGCCTCCAGAggctggatg gtgggttggg	Cloning
GFP_Fw-A593	cccaacccaccatccagccTCTGGAGGCGGCGGATCTatggtgag caagggcgagga	Cloning
GFP_Rv-A593	cgccaatgatccagccagacacTGAGCCTCCTCCGCCTGActtgtac agctcgtccatgccg	Cloning
BAK1_Fw2-A593	cggcatggacgagctgtacaagTCAGGCGGAGGAGGCTCAgtgtc tggctggatcattggcg	Cloning
BAK1_Attb1	GGGGACAAGTTTGTACAAAAAAGCAGGCTATatggaa cgaagattaatgatcccttgc	Cloning
GFP_attB_Rv	TACCCAGCTTTCTTGTACAAAGTGGTCCCCttacttgtaca gctcgtccatgccg	Cloning
pOPINM_BAK1-Fw	AAGTTCTGTTTCAGGGCCCGCTTGGTGGCGAAGGA AA	Cloning
pOPINM_BAK1-Rv	ATGGTCTAGAAAGCTTTATCTTGGACCCGAGGGGT ATTC	Cloning
INM-BAK1-S612A-Rv	ATGGTCTAGAAAGCTTTATCTTGGACCCGCGGGGT ATTC	Cloning
INM-BAK1-AAA-Rv	ATGGTCTAGAAAGCTTTATCTTGGACCCGAGGGGT ATTCGTTTTCGATCTGGGCAGCGGCATCGCCAATGA TC	Cloning
PEPR1KDBAMHIFw	AAAAAGGATCCccTCTTTGTTGTTGAACAAAGTTCT TGCAG	Cloning
PEPR1KDECORI-Rv	TTTTTGAATTCTTACCGAACTGAATCAGAGGAGC	Cloning
PEPR1_Km-K855E_Fw	gaaaggtctacgctgtggagagacttgtattcgcg	Cloning
PEPR1_Km-K855E_Rv	cgcgaatacaagtctctccacagcgtagacctttc	Cloning
BIK1-Km_KK105AA_Fw	GTCATCGCCGTTGCAGCGCTTAACCAAGAA	Cloning
BIK1-Km_KK105AA_Rv	TTCTTGGTTAAGCGCTGCAACGGCGATGAC	Cloning
BAK1-Km_D416N-Rv	cagctttcacatTtcgatgaataatctttgg	Cloning
BAK1-Km_D416N-Fw	attattcatcgaAatgtgaaagctgcaaata	Cloning
BAK1-5_C408Y_Fw	ttacatgatcattAcgacccaaagattattcatc	Cloning

BAK1-5_C408Y_Rv	aatctttgggtcgTaatgatcatgtaaatac	Cloning
BIK1-AttB1-Fw	GGGGACAAGTTTGTACAAAAAAGCAGGCTCAATGG GTTCTTGCTTCAGTTCTCGA	Cloning
BIK1 _wo_stop-AttB2-Rv	GGGGACCACTTTGTACAAGAAAGCTGGGTACACAA GGTGCCTGCCAAAAGGTTT	Cloning